Electron Microscopy

Research School
“Imaging of 3D-structures”

Prof. Dmytro Orlov, Division of Materials Engineering, LTH
dmytro.orlov@material.lth.se

Acknowledgements

1. Prof. Stefan Zaefferer, Max-Planck-Institut für Eisenforschung, Düsseldorf, Germany;
2. Prof. Reine Wallenberg, Director of nCHREM, LU, Sweden.

Microstructure of crystalline materials as a subject

1. Microstructure of crystalline materials can be considered as a regular arrangement of atoms into a crystal lattice.
2. The lattice has defects at various scales disturbing the perfect order and therefore significantly affecting most structural and functional properties.
3. The analysis of defects is typically the main subject of electron microscopy based analysis. Of particular interest in 3D microscopy are
    1. 1D (line) defects: dislocations;
    2. 2D (planar) defects: stacking faults, anti-phase boundaries, grain and phase boundaries;
    3. 3D (volume) defects: precipitations, voids, cracks.

Characteristics of ‘light’ sources

Source	*Brightness (particles/sR/eV)*	*Elastic Mean Free Path (nm)*	*Absorption Pathlength (nm)*	*Attainable Probe Size (nm)*
Neutrons	10^{14}	10^{7}	10^{8}	10^{4}
X-rays / photons	10^{26}	10^{3}	10^{5}	$\sim 3\text{x}10^{1}$
Electrons	10^{29}	10^{1}	10^{2}	$< 10^{-1}$

Optical vs Electron Microscopy

	Light Microscope	**Scanning Electron Microscope (SEM)**	**Transmission Electron Microscope (TEM)**
Imaging Source	**Photons**	**Electrons**	**Electrons**
Wavelength,	**300-700 nm**	**≤ 1 nm**	**≤ 1 nm**
Resolution	**200 nm**	**1-10 nm**	**≤ 1 Angstrom**
Magnification	**~1,000x**	**1,000,000x**	**< 50,000,000x**
Sample Types	**Living/Dead**	**Solid** **Conductive** **Vacuum Compatible** **< 25mm diameter** **(typically)**	**Solid** **Conductive** **Vacuum Compatible** **3mm diameter** **< 100nm thick**
Information Provided	**Surface Topography, Structure, Morphology**	**Surface Topography, Morphology, Composition, Orientation**	**Internal Structure, Composition, Orientation**

Depth of Focus/Field

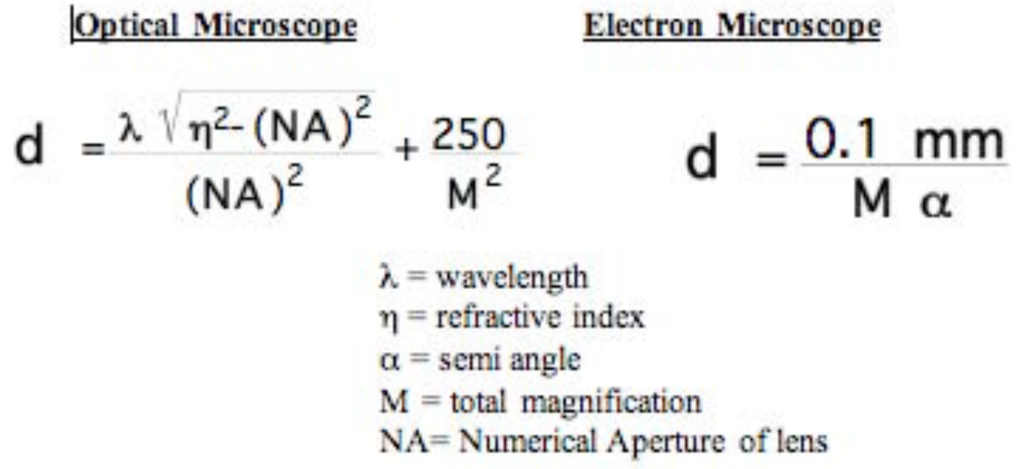

Optical Microscope

$$d = \frac{\lambda \sqrt{\eta^2 - (NA)^2}}{(NA)^2} + \frac{250}{M^2}$$

Electron Microscope

$$d = \frac{0.1 \text{ mm}}{M \alpha}$$

λ = wavelength
η = refractive index
α = semi angle
M = total magnification
NA= Numerical Aperture of lens

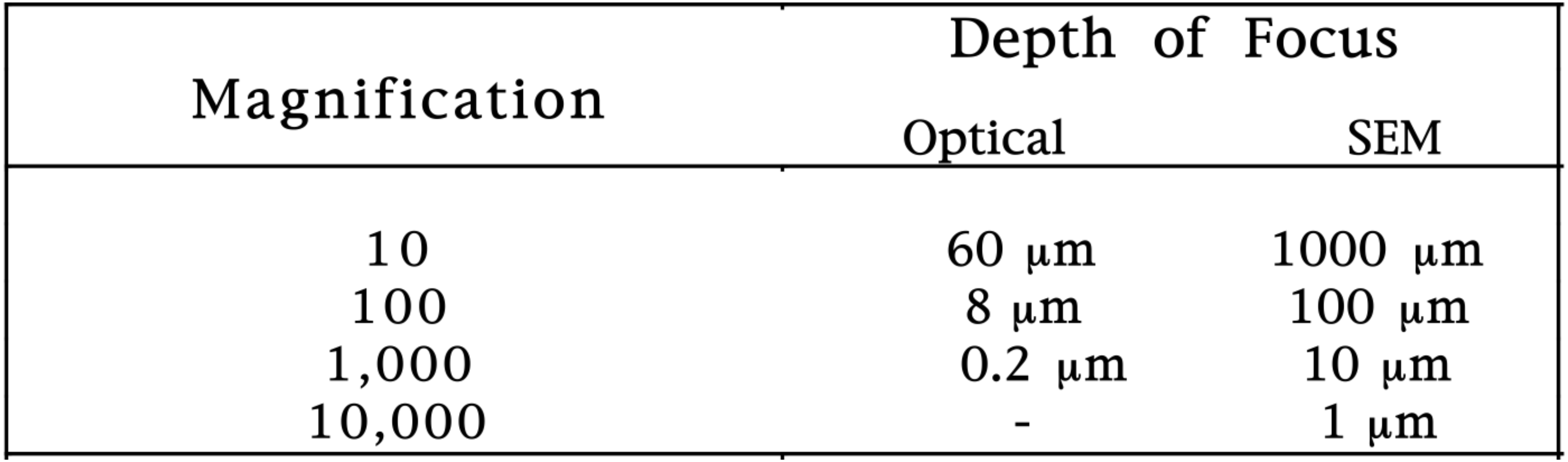

Magnification	Depth of Focus	
	Optical	SEM
10	60 μm	1000 μm
100	8 μm	100 μm
1,000	0.2 μm	10 μm
10,000	-	1 μm

History of EM development

1897 JJ Thompson - Discovery of the Electron

1926 H. Bush Magnetic/Electric Fields as Lenses

1929 E. Ruska PhD Thesis Magnetic lenses

1931 Knoll and Ruska 1st EM built

1932 Davisson and Calbrick - Electrostatic Lenses

1934 Driest & Muller - EM *surpases LM*

1939 von Borries & Ruska - 1st Commercial EM
~ 10 nm resolution

1945 ~ 1.0 nm resolution (Multiple Organizations)

1965 ~ 0.2 nm resolution (Multiple Organizations)

1968 A. Crewe - U.of Chicago - Scanning Transmission Electron Microscope
~ 0.3 nm resolution probe - *practical Field Emission Gun*

1986 Ruska et al - Nobel Prize

1999 < 0.1 nm resolution achieved (OÅM)

2009 0.05 nm (TEAM)

Optical vs Electron Microscopes

LM

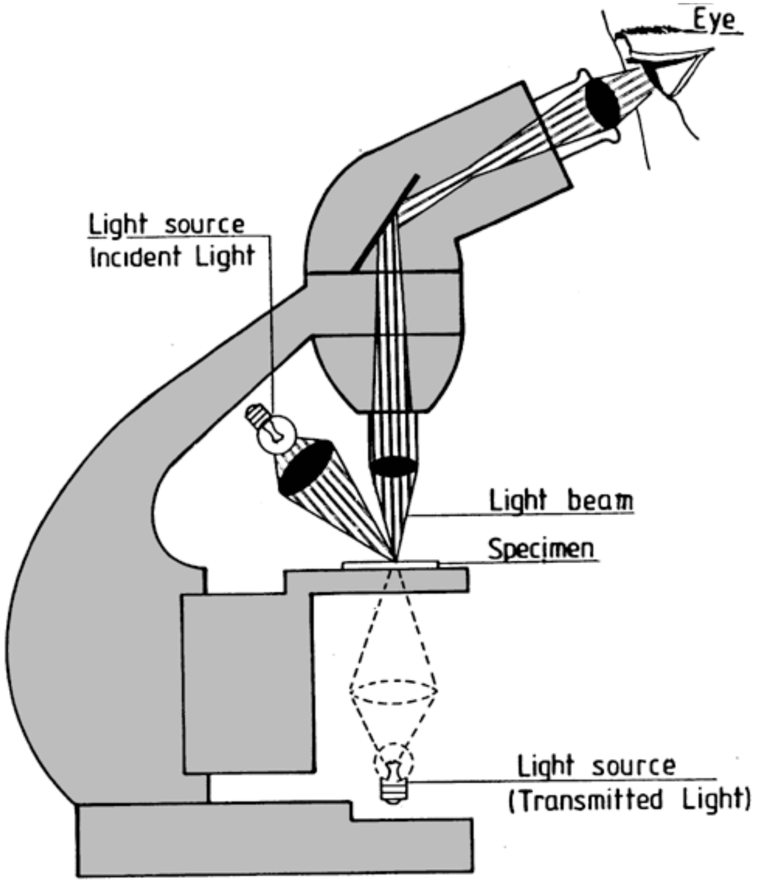

TEM

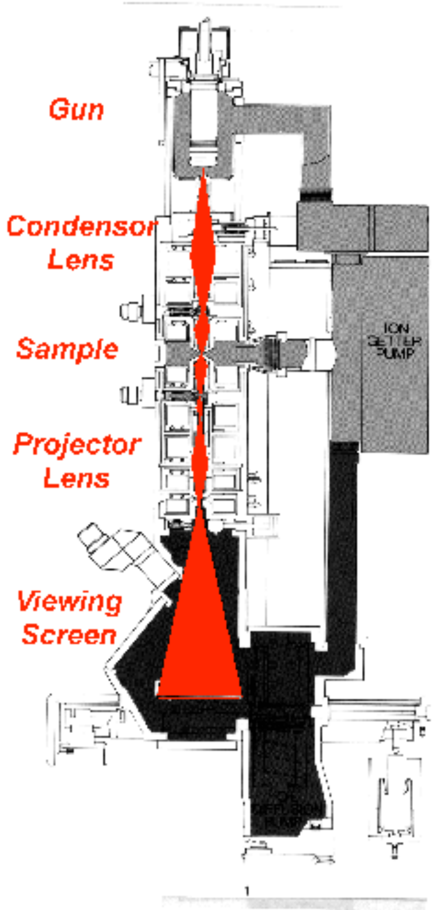

SEM

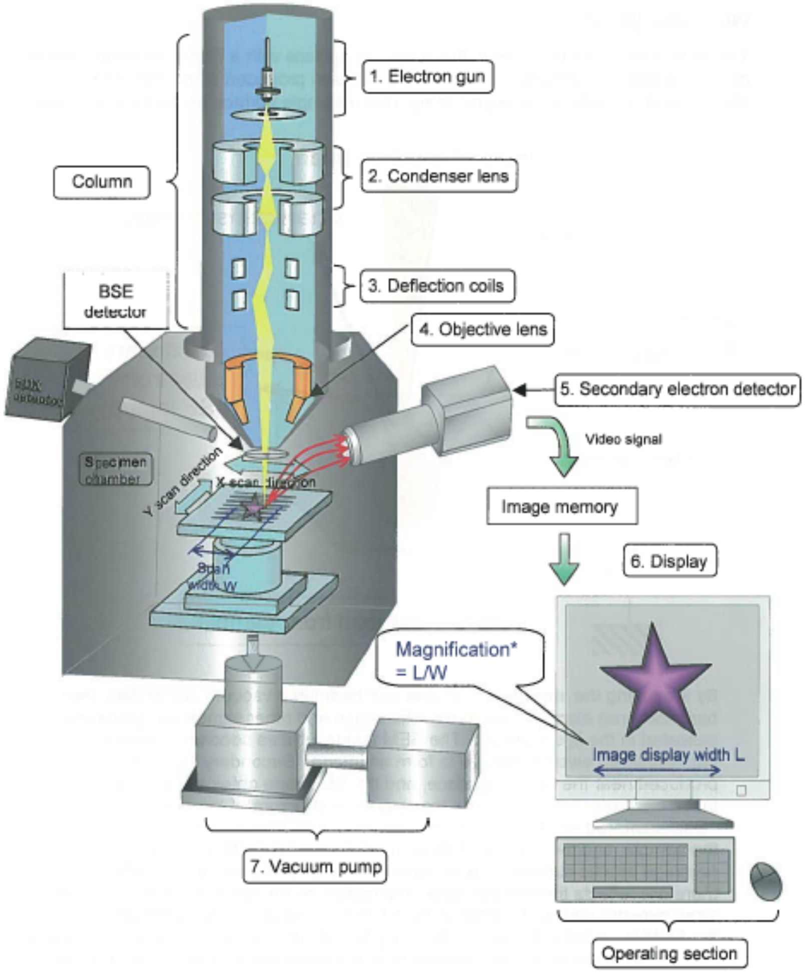

Optical vs Electron Microscopes

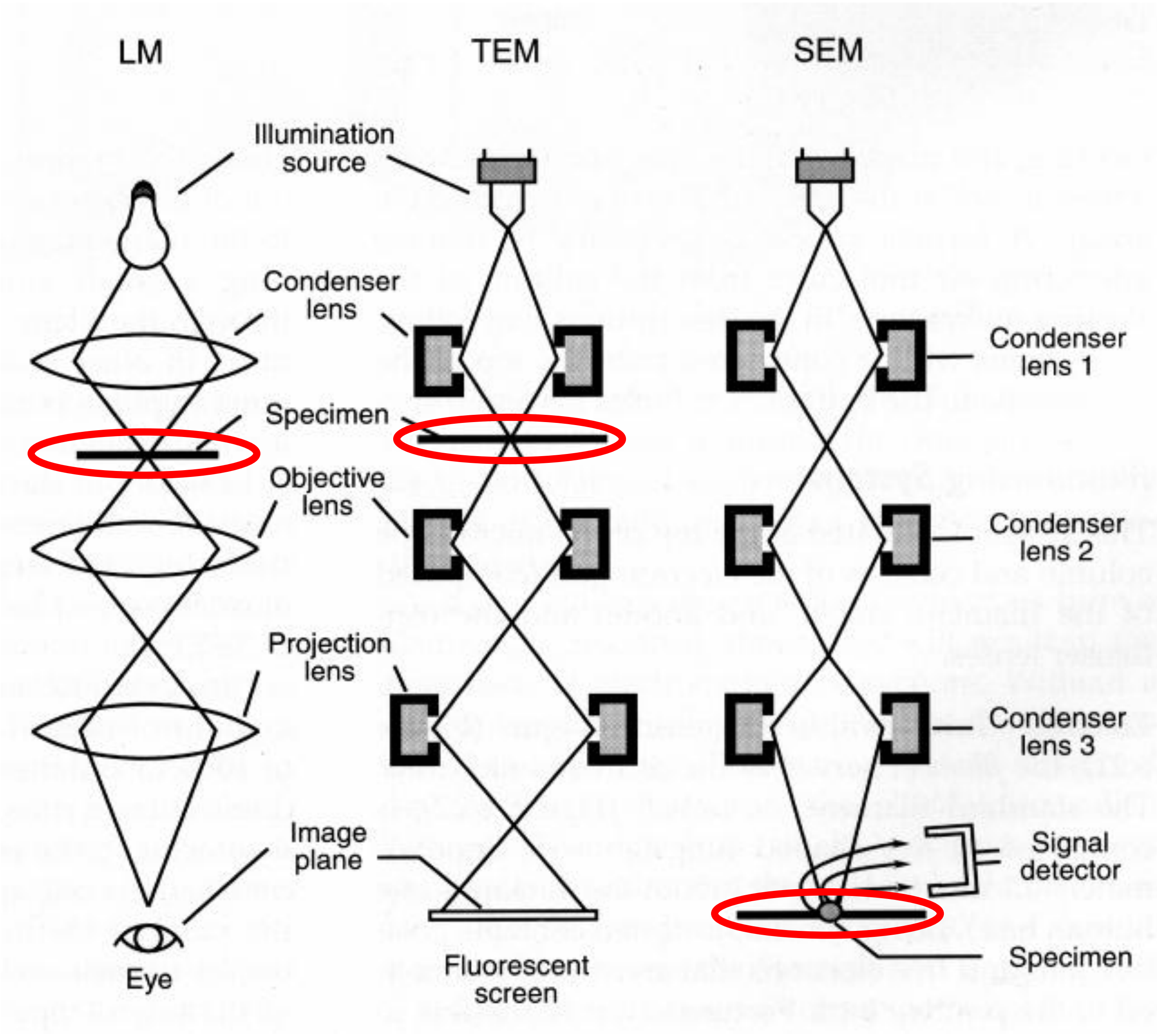

Comparison of electron and X-ray properties (for SEM)

Property	Electron	X-ray (photon)
Mass	$9.11\text{x}10^{-31}$kg (matter)	None (electromagnetic radiation, λ 10 to 0.01nm)
Charge	$-1.60\text{x}10^{-19}$C	None
Speed	Determined by energy	Speed of light in medium
Absorption	Many mechanisms, frequent scattering in matter results in loss of energy and/or change in direction	Approximation: X-rays travel in a straight line until they are destroyed in a single absorption event (the photoelectric effect)
Diffraction and refraction	Yes	Yes
Magnetic field	Changes direction	No effect
Electric field	Changes energy and/or direction	No effect

Electrons: In the SEM, electrons are usually described in terms of their energy (*E*) given in electron-volts (eV) where: 1 eV = $1.6\text{x}10^{-19}$ J

X-rays: described either by their energy *E* (eV) or by their wavelength λ (nm):
λ(nm) = 1239.6/*E* (eV), i.e. an X-ray with 0.1nm wavelength has an energy of 12,396 eV

Comparison of SEM and TEM

Scanning Electron Microscope

- Accelerating voltage: 0.1 to 40 kV,
  typically 5 to 25 kV for metallic materials
  (limits range of X-ray energies excited).
- Beam current: 0.01nA to >3000nA,
  typically around 1nA
  (limits X-ray count-rate).
- Probe size: <1nm to >1000nm,
  typically around 50nm
  (typically much smaller than the width of the volume of X-ray generation in a bulk sample).
- Bulk sample, typically around 25mm diameter, polished (sometimes coated).

Transmission Electron Microscope

- Accelerating voltage: 100 to 300 kV ,
  typically 200 kV for metallic materials
  (can excite almost all X-ray energies).
- Beam current: 0.01nA to >5nA,
  typically around 1nA
  (limits X-ray count-rate).
- Probe size: <0.1nm to >100nm,
  typically around 10nm
  (will often limit spatial resolution).
- Thin-film sample 3mm diameter and analysis area <100nm thick.

‘Light’ source in EM

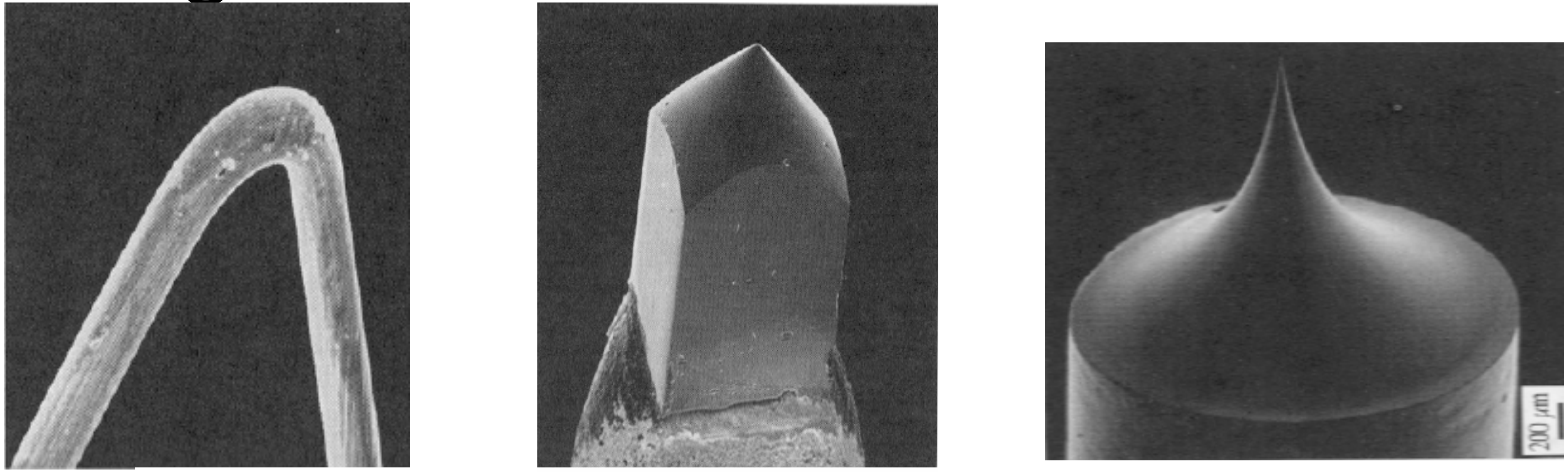

	W	LaB_6	FEG (Schottky)
Maximum Current (nA)	1000	500	300
Normalised Brightness (-)	1	10-30	2500
Energy spread (eV)	3-4	1.5-3	0.6-1.2
Source spotsize	30-100 μm	5-50 μm	15-30 nm
Required Vacuum (Pa)	10^{-3}	10^{-5}	10^{-7}
Temperature (K)	2700	2000	1800
Life time (hr)	60-200	1000	>2000
Normalised Price (-)	1	10	100

‘Light’ source in Electron Microscopes

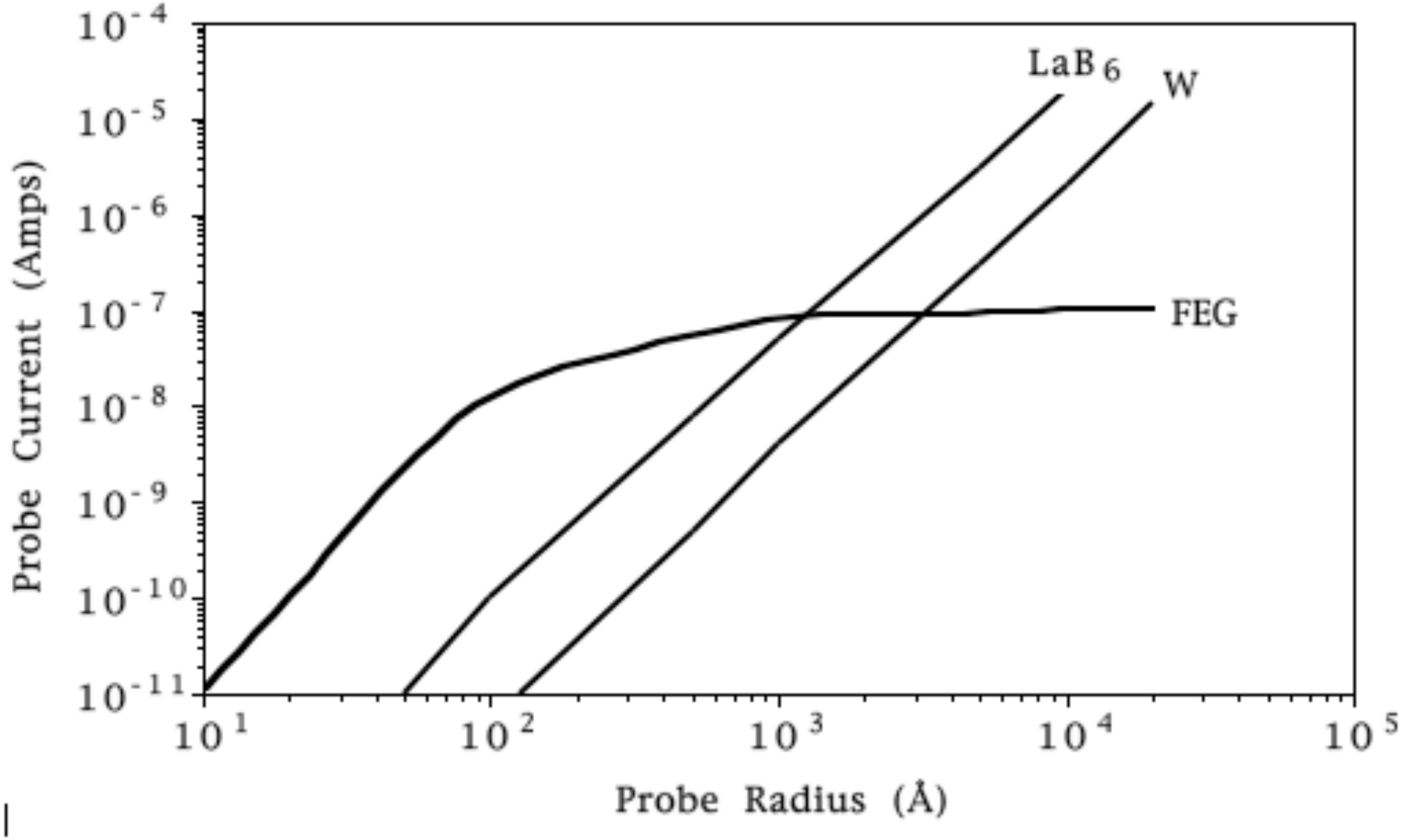

Electron Beam Scattering

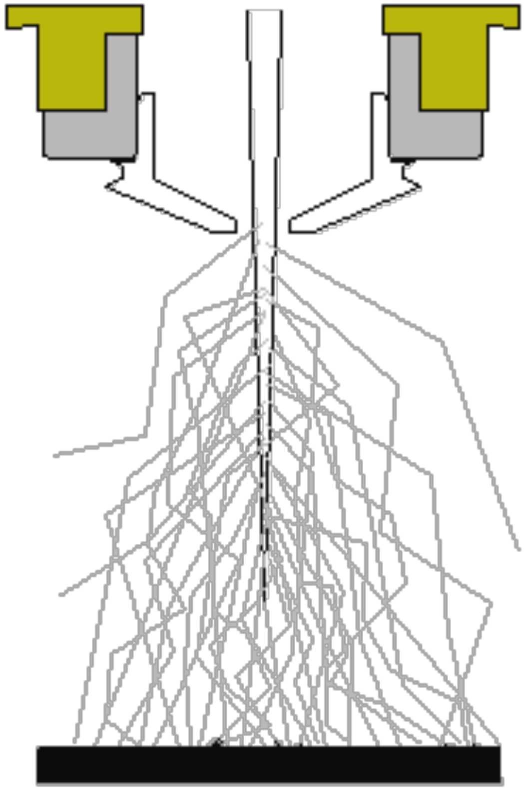

Air
(scattered completely)

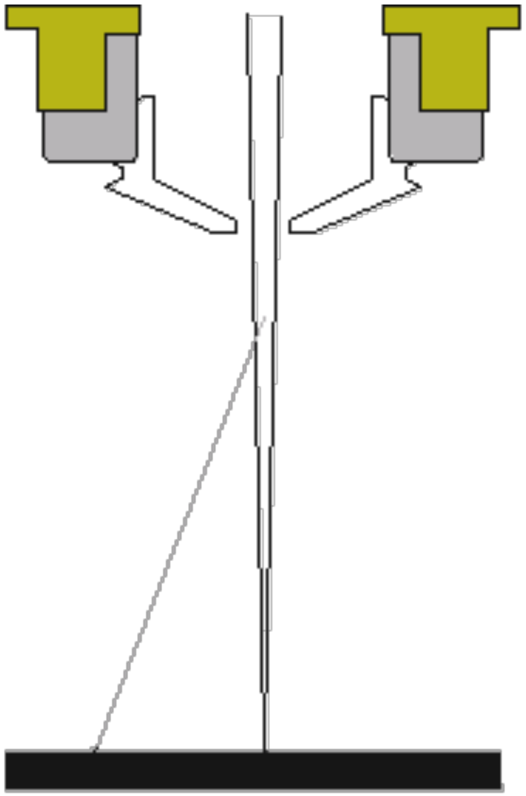

Vacuum
(no scattering)

The Gaseous Environment

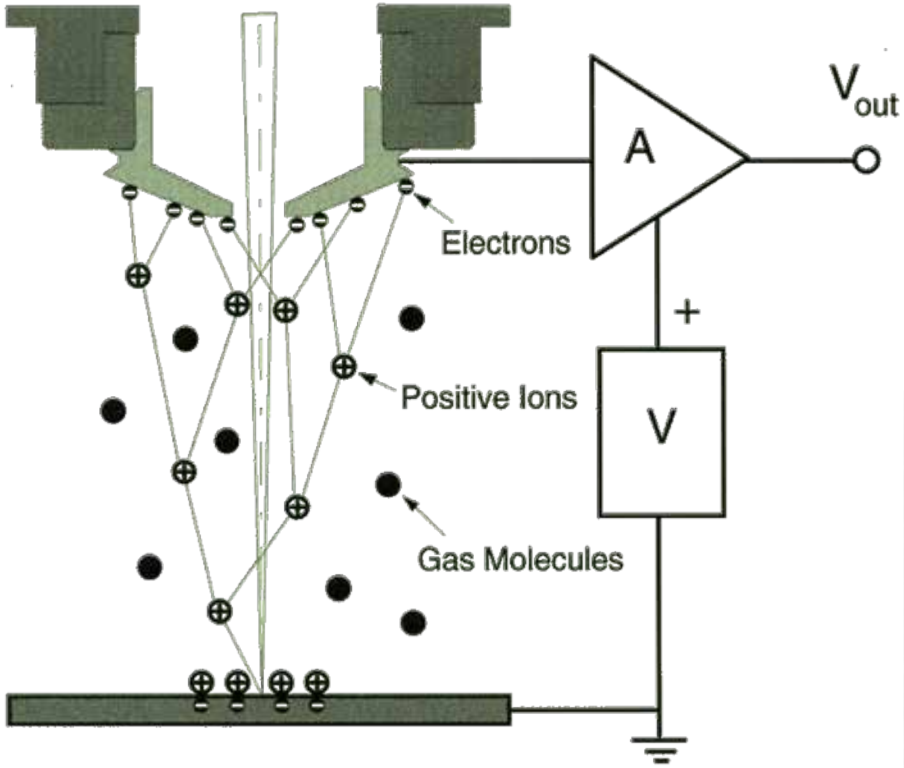

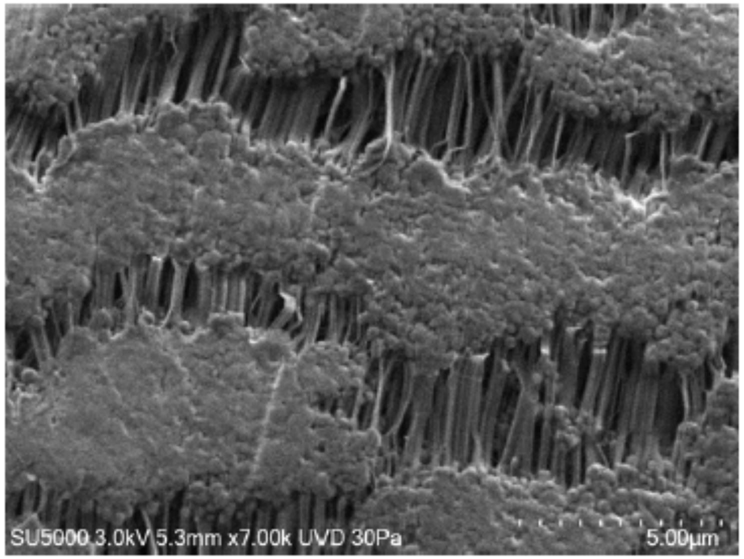

Accelerating Voltage: 3 kV, Variable Pressure, 30 Pa, UVD
Magnification: 7,000 x, Sample: PTFE

Local charge compensation

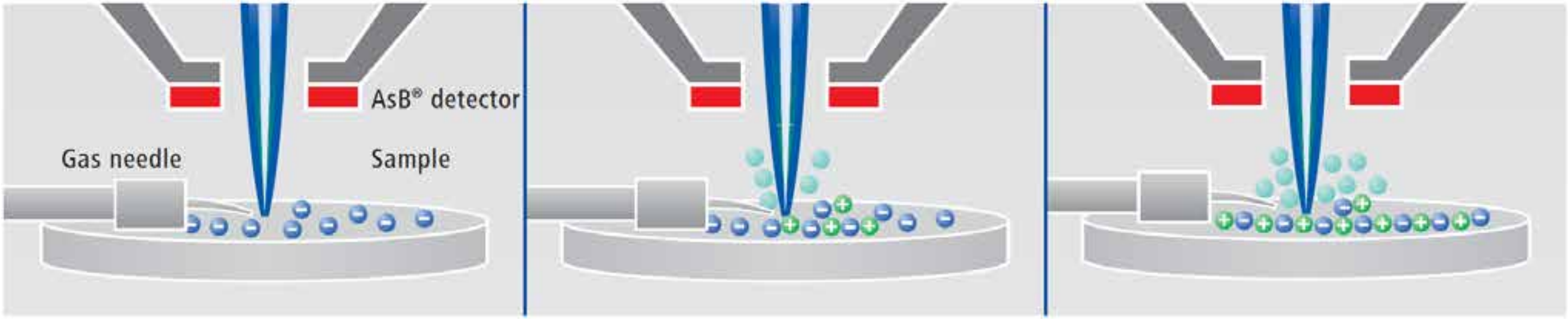

Fig. 3: Principle of charge compensation:
Left: The sample surface of an insulator charges up due to electron irradiation.
Middle: When the nitrogen flow is turned on, the gas molecules (light green) form a local gas cloud above the sample surface.
Right: SE and BSE emitted from the sample surface ionize the gas molecules. As the resulting positive ions (dark green) hit the sample surface it is neutralized. Full imaging and analytical capabilities are thus enabled.

The National Center for High Resolution Electron Microscopy

nCHREM

Lund University

JEOL 3000F AEM Yr 2000

JEM 2200FS Cryo 2016

JSM 6700/ SEM/EDS

Hitachi 3300 ETEM 2016

Nanofactory STM

Acknowledgement: The Knut and Alice Wallenberg Foundation

The National Center for HREM, LTH, Lund University, Reine Wallenberg

Gases and MO:s

1. nitrogen
2. Trimethylindium
3. Trimethylaluminium
4. trimethylgallium
5. Hydrogen
6. Trimethylantimony
7. Phosphine
8. Arsine
9. Oxygen

What can we achieve with the new ETEM?

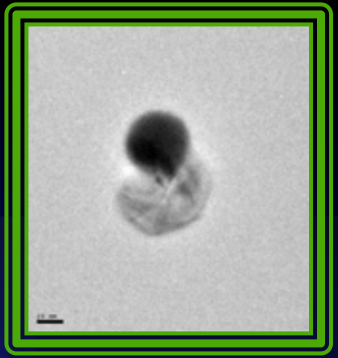

Study the birth of a nanowire

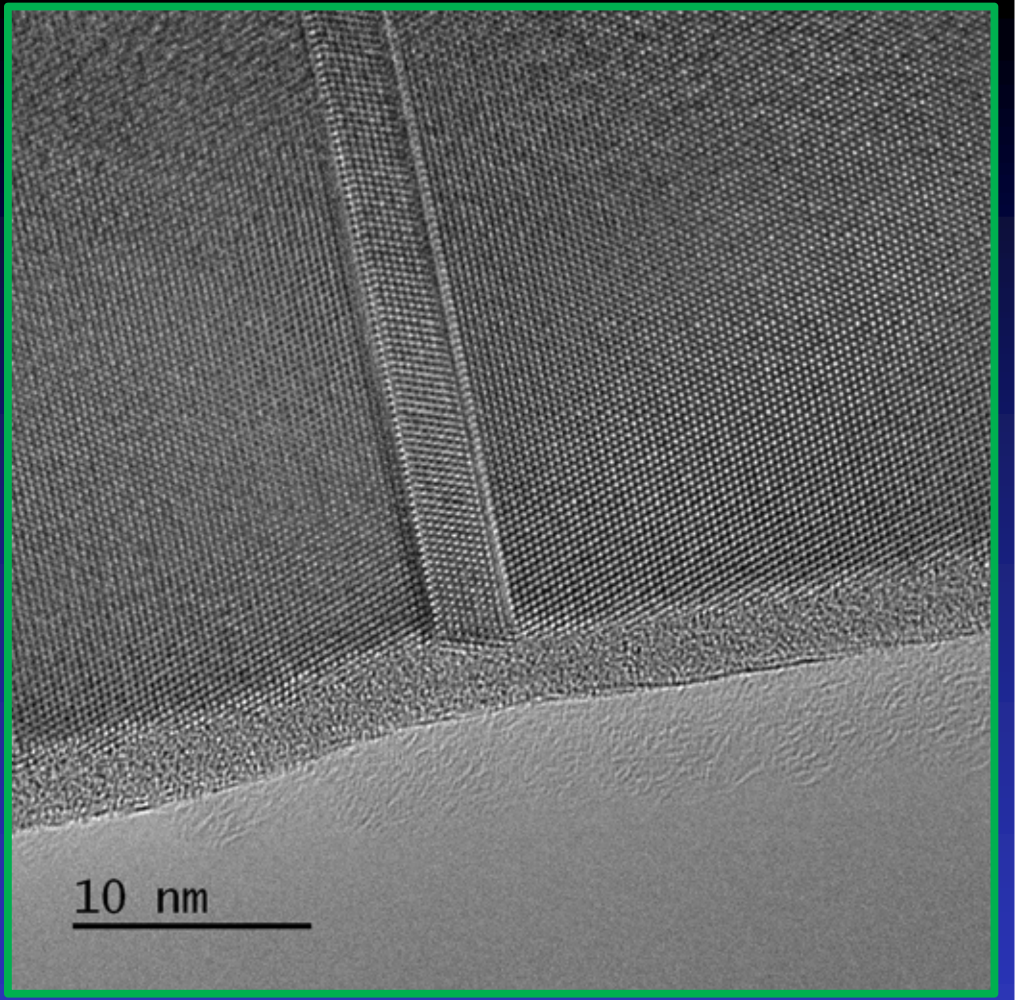

- High-resolution transmission imaging during growth
- Simultaneous chemical analysis

..and outer 3-D surfaces by secondary electron detector

Aerotaxy – the principle

Au seed particles generated in gas stream, mix with gases and pass through oven (1 second) – Nanowires!

- No substrate
- Grows 1 μm s^{-1} (43 M atoms/s)
- Continuous

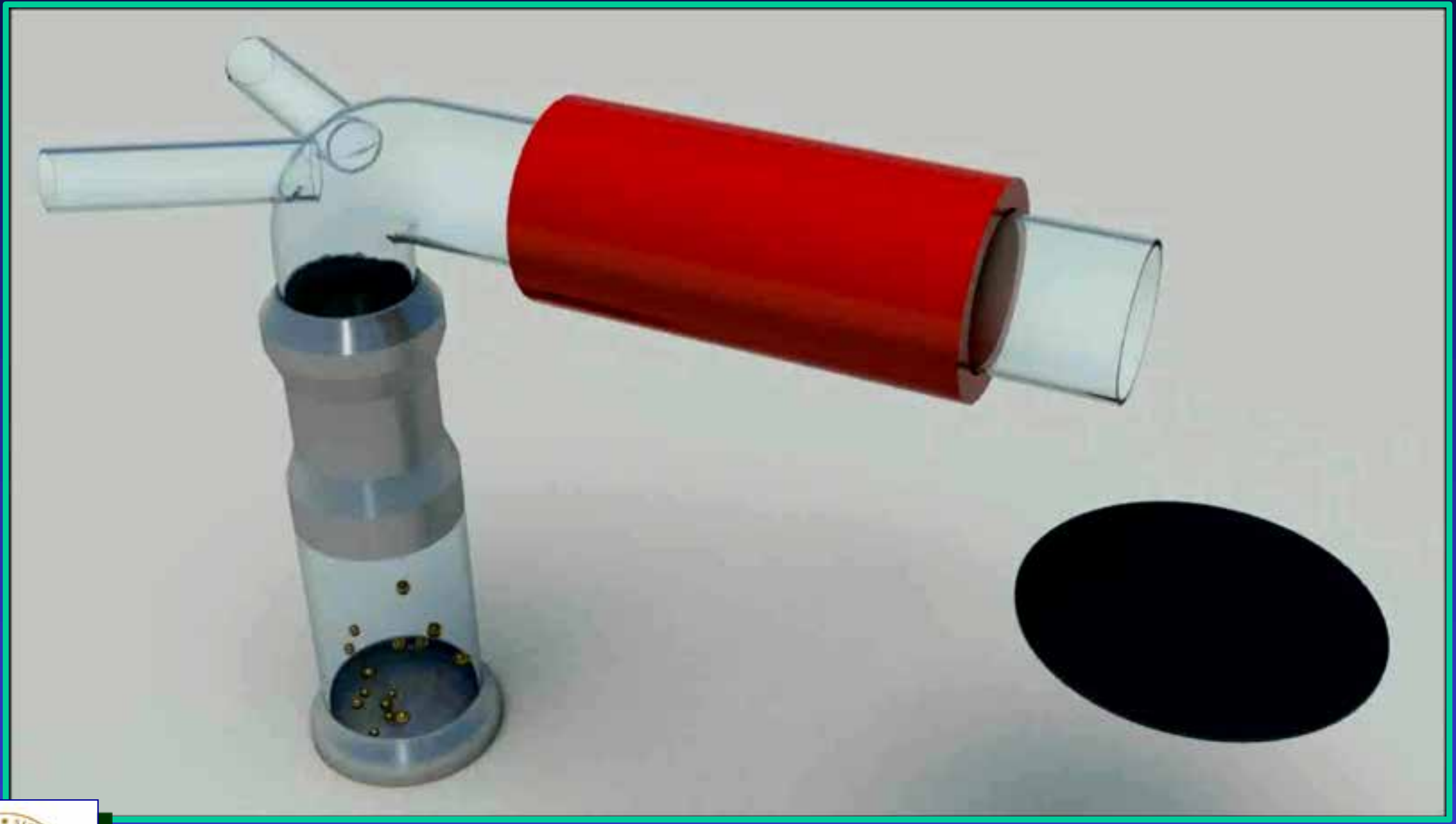

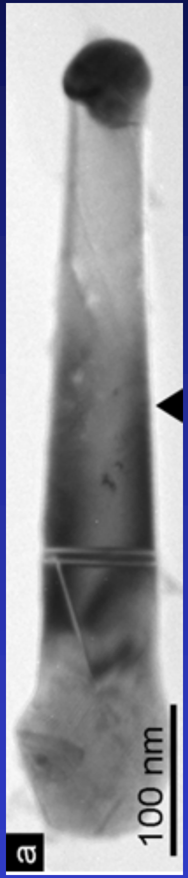

Heurlin M , et al. ***Nature*** **492** (2012) 90. Continous gas-phase synthesis …

Doping GaAs NWs with higher Sn renders buds on the surface

Nanowire – Tiltseries - Tomography

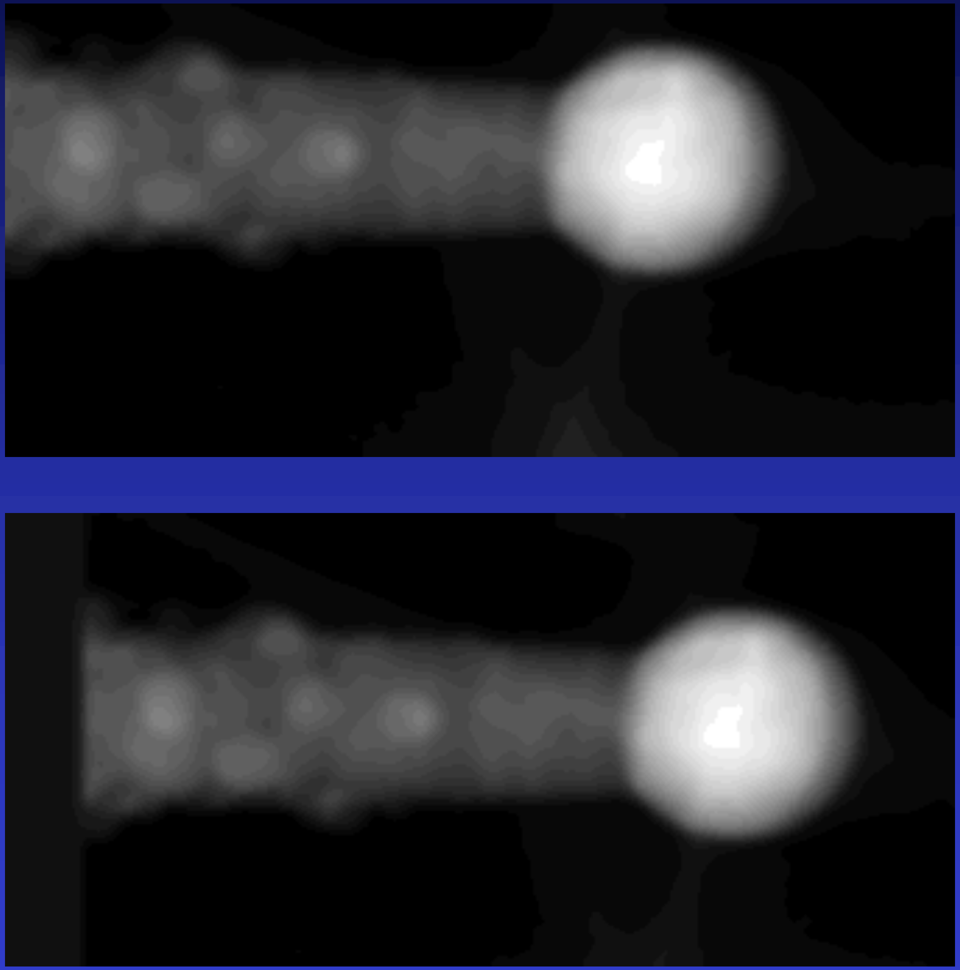

- 133 images manually acquired

  (by Axel Persson)

- Covering 136°

  (missing wedge: 44°)

- STEM – HAADF images (density)

Tomogram by
Axel Persson

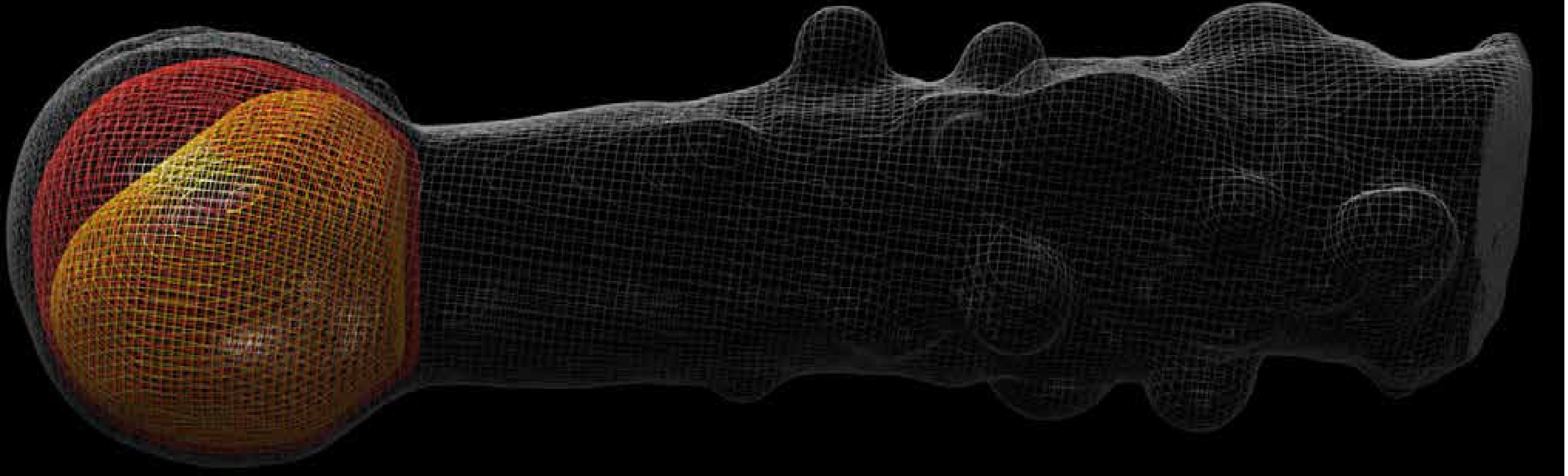

3-D tomogram, voxel size 1 nm^3
Sectioning by density

Identification of the different parts by XEDS mapping

- Sn dopant conc. In the wire $10^{18} – 10^{19}$ cm^{-3} - too low for XEDS detection – BUT large agglomerate in seed particle

- Surface particles -pure Ga

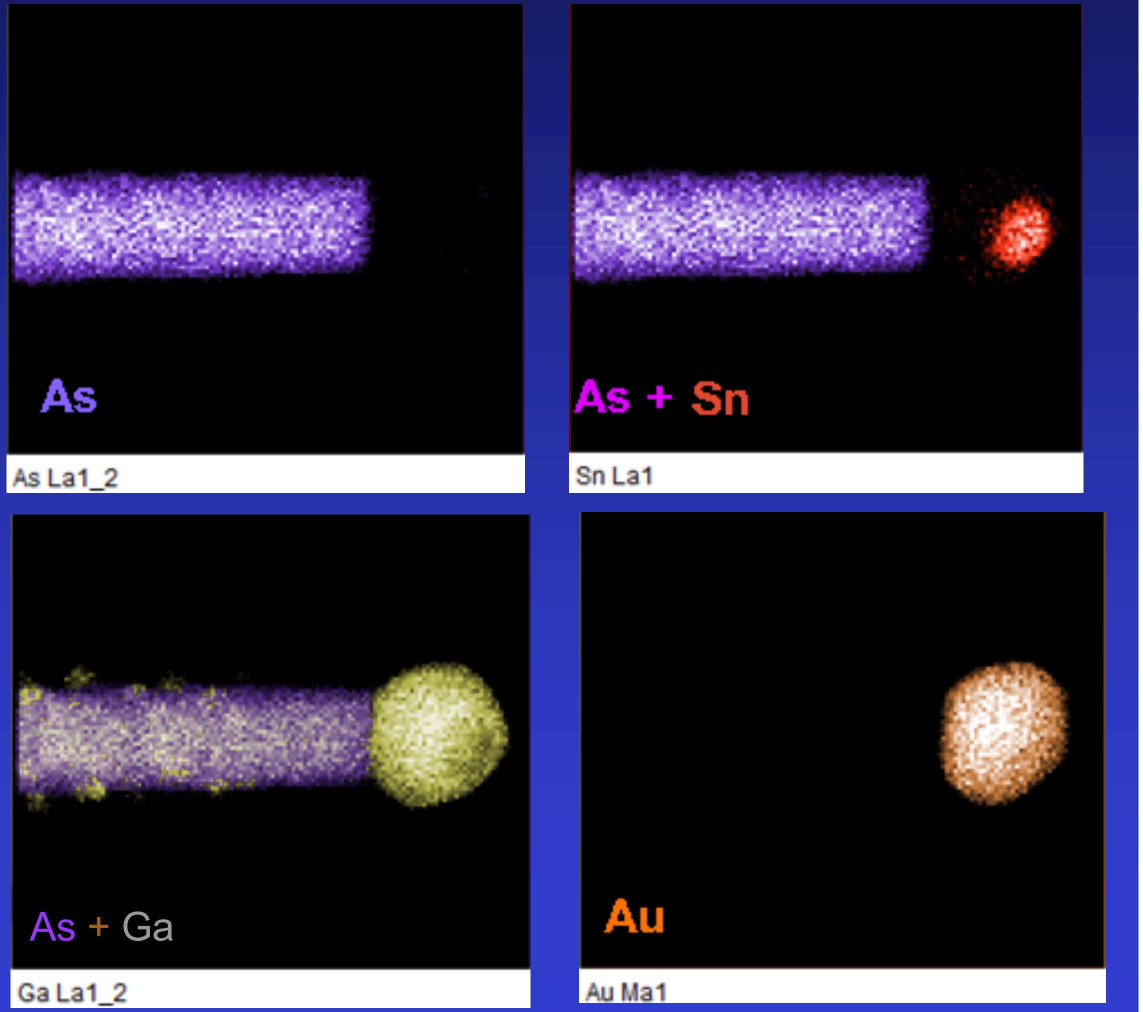

GaAs nanowire XEDS image
Au-seeded
Sn-doped

Electron tomography at nCHREM

NANO MICRO small

Full Paper

Electron Tomography Reveals the Droplet Covered Surface Structure of Nanowires Grown by Aerotaxy

First published: 12 July 2018

A R Persson, W Metaferia, S Sivakuhmar, L Samuelson, M Magnusson, L R Wallenberg

https://doi.org/10.1002/smll.201801285

- n-doping by Sn possible for GaAs in aerotaxy process – at lower levels.
- Higher levels gives surface Ga buds – may be used for branch growth.
- New method, *Azimutal Mapping,* reveals ordering of buds.

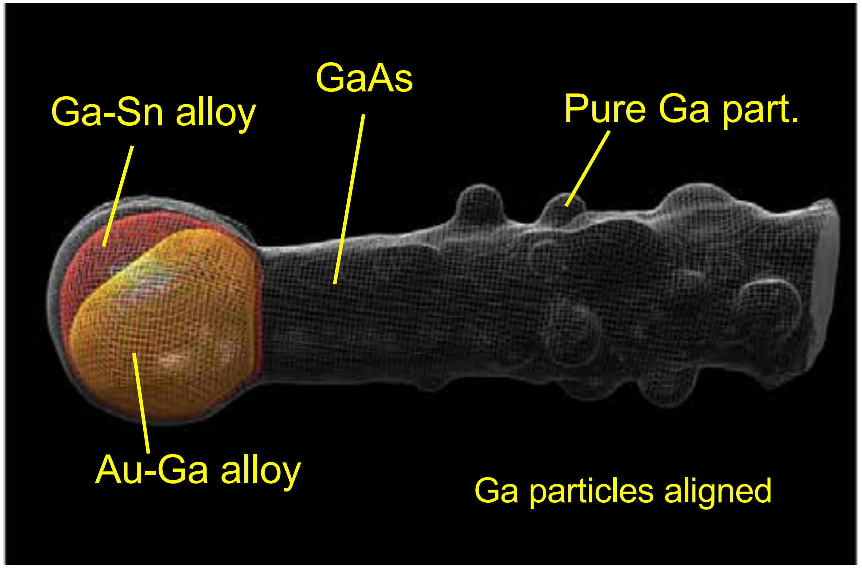

3-D tomogram, voxel size 1 nm^3

Sectioning by density

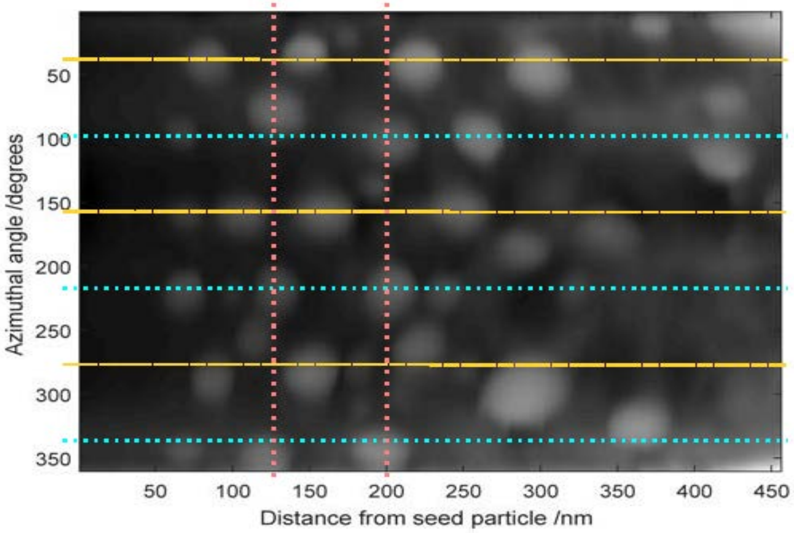

In-situ generated Ga buds can be used for growing secondary branches on nanowires

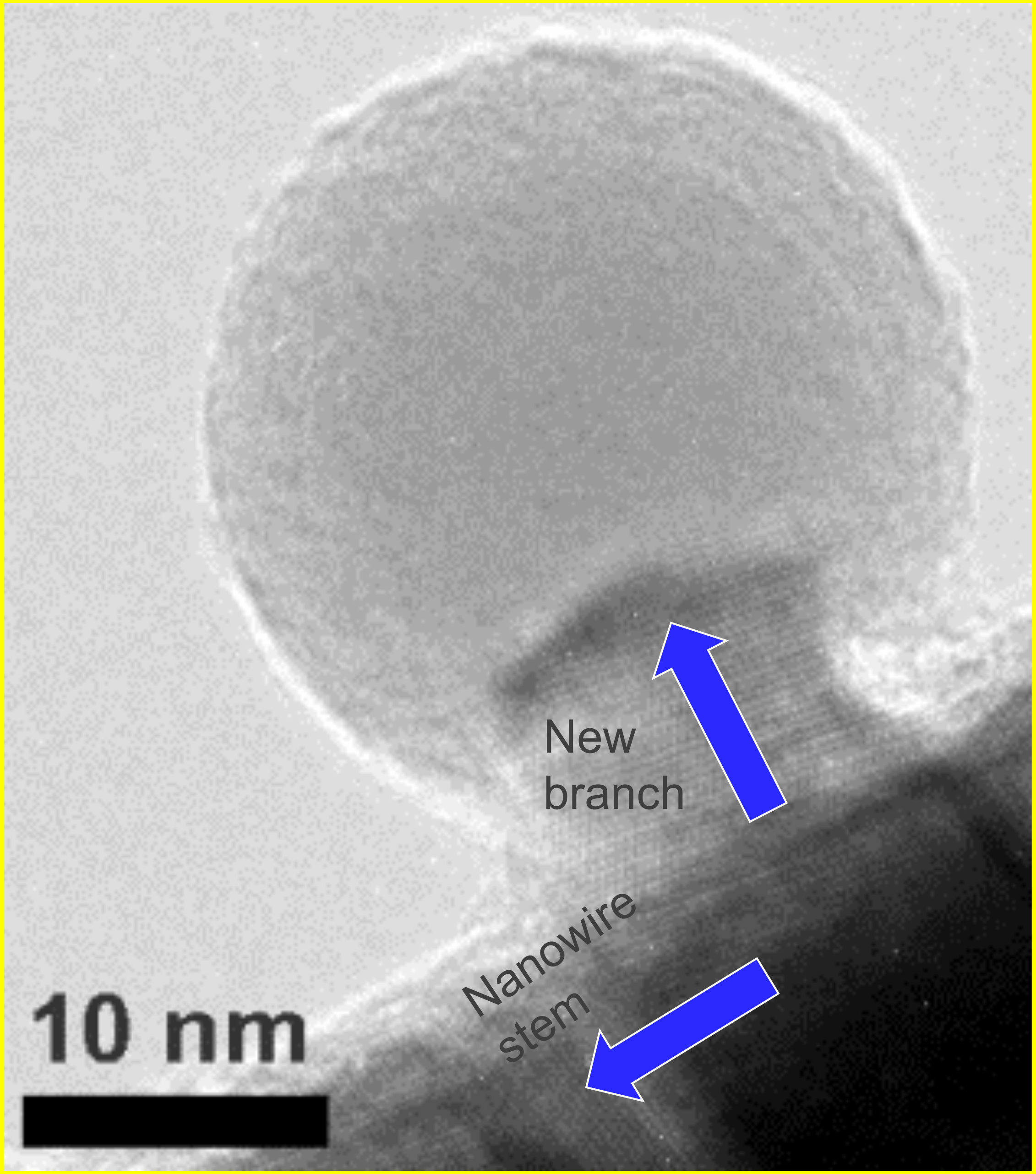

GaAs nanowire HREM image
Au-seeded
Sn-doped

Skinning the nanowire!

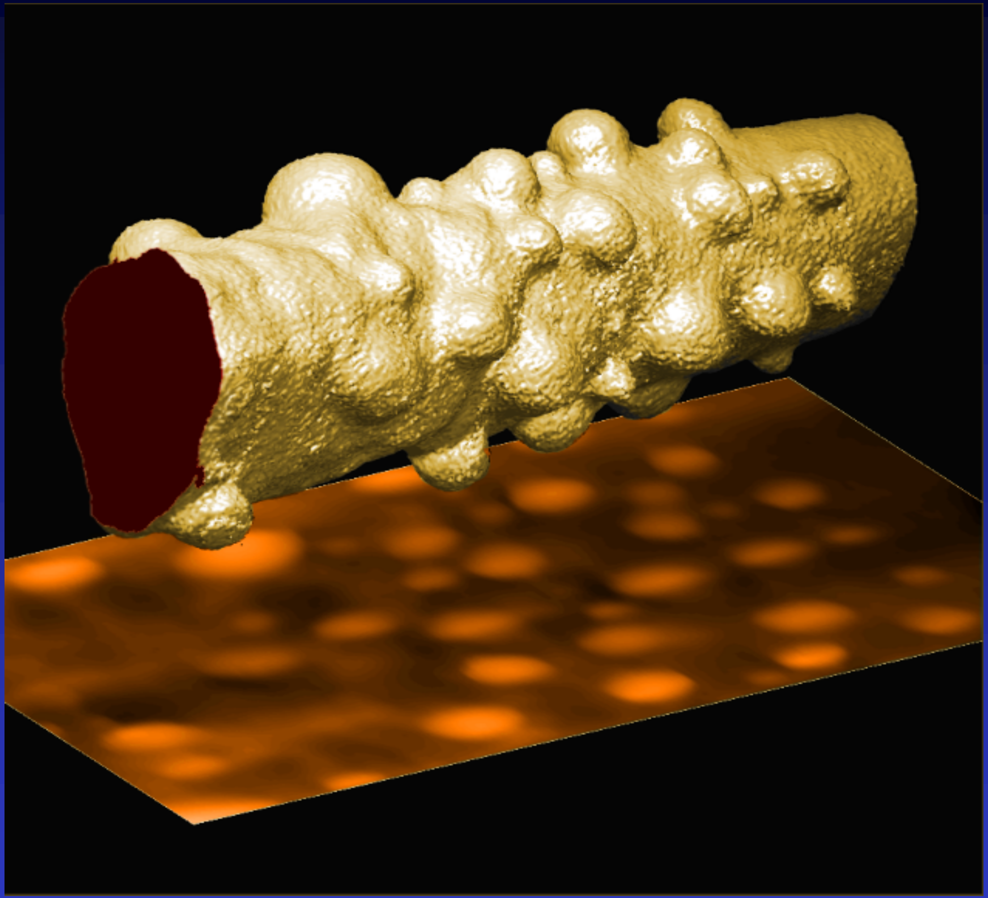

Azimutal mapping correlates particle growth with crystallographic direction

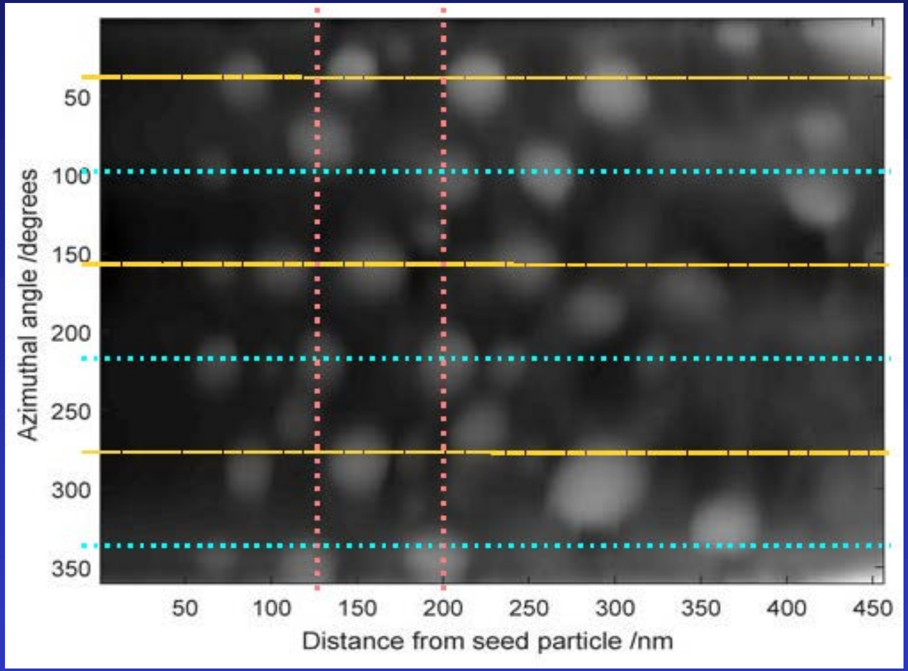

Complex 3-D nanowire structures revealed by electron tomography

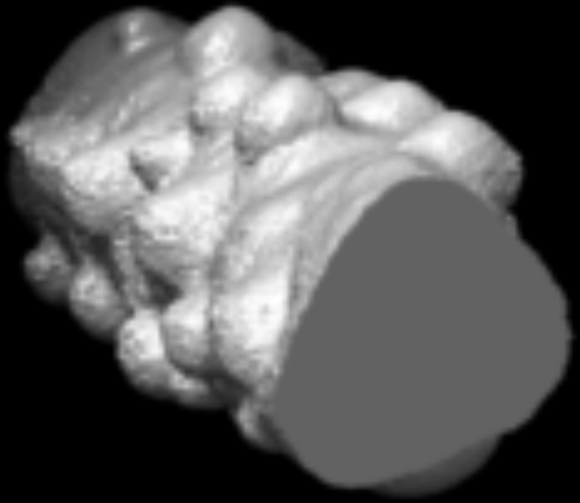

The National Center for HREM, Lund University, Reine Wallenberg

Dislocations interacting with precipitate - tomogram

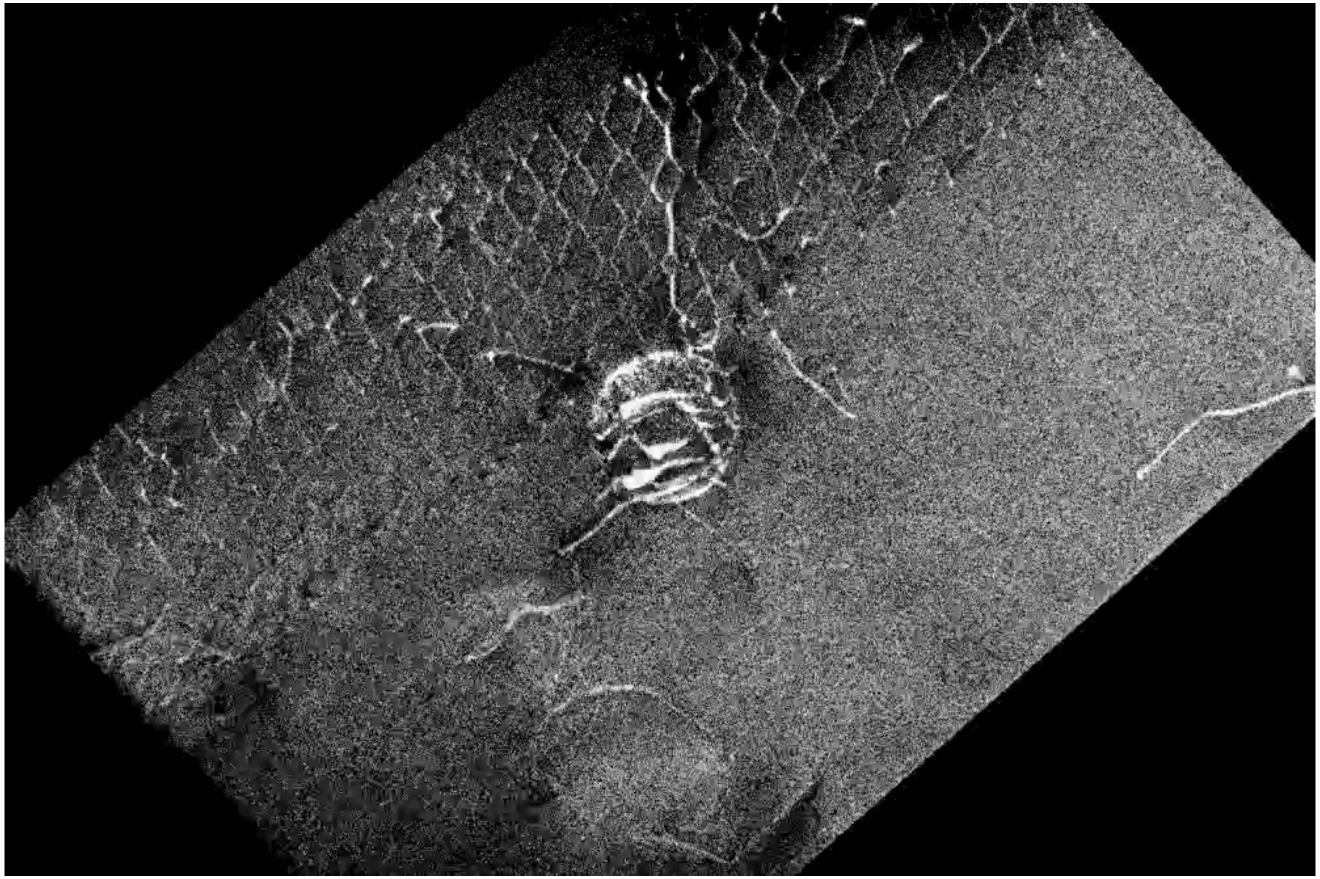

3D reconstruction from weak-beam dark-field series of images acquired over the angular range from −21.3° to +37.3° with the diffraction condition maintained with **g** = 020 and $\mathbf{s}_g = 6.7 \times 10^{-3}$ Å^{-1}.

[G.S. Liu and I.M. Robertson, J. Mater. Res., Vol. 26, No. 4, Feb 28, 2011]

Dislocations interacting with precipitate- tomogram

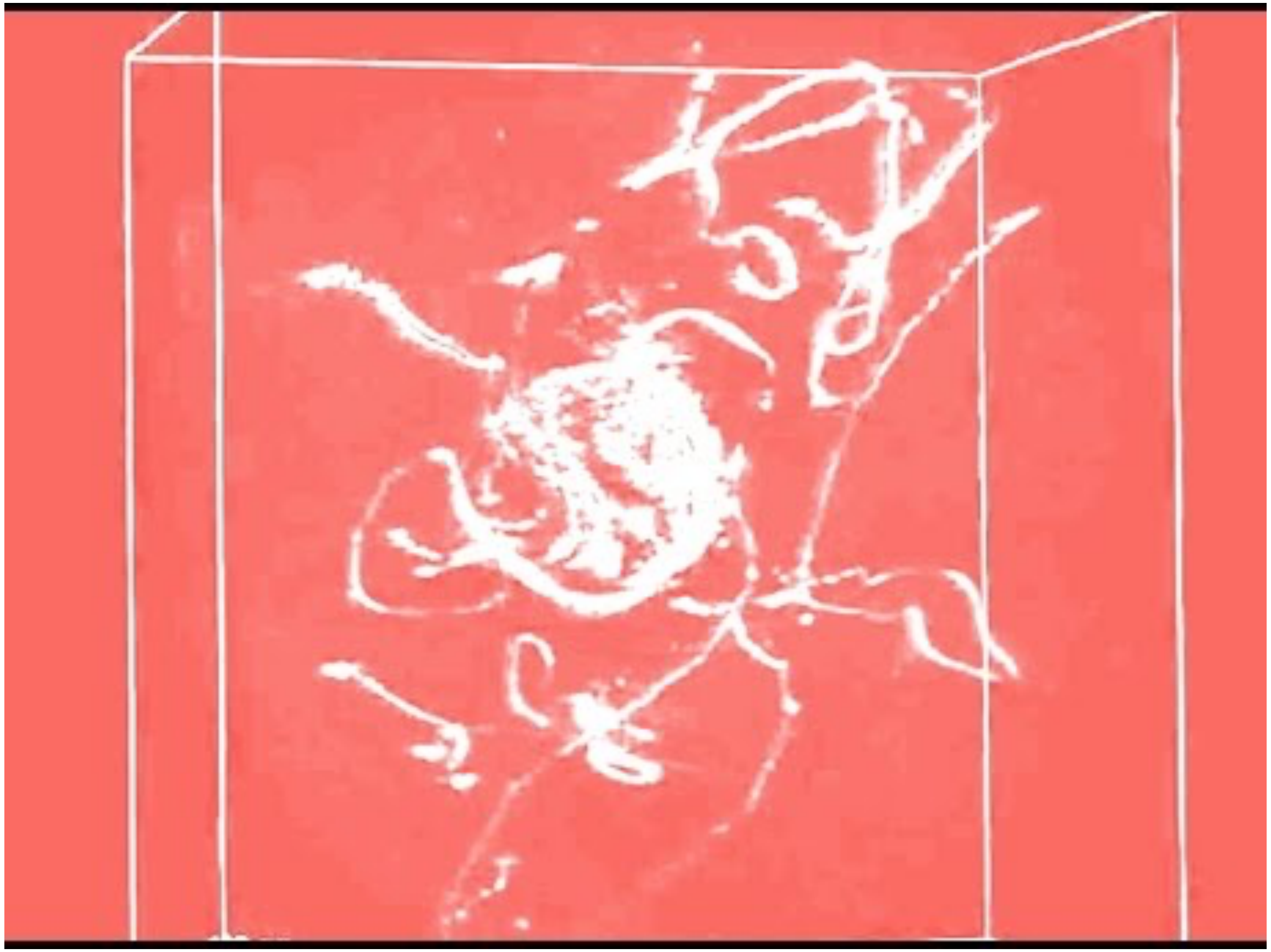

Dislocation interactions with an Al_3Sc particle in an Al–Mg–Sc alloy. Weak-beam dark-field images were acquired every one degree over an angular range of -28 to +32 degrees (X-tilt only) while maintaining a constant deviation parameter and diffraction vector

[https://www.youtube.com/watch?v=kuBV92aLvbI]

Dislocations interacting with precipitate - analysis

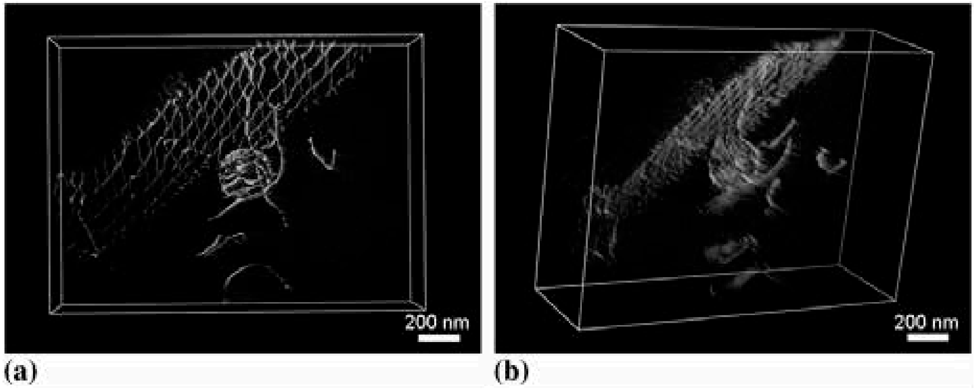

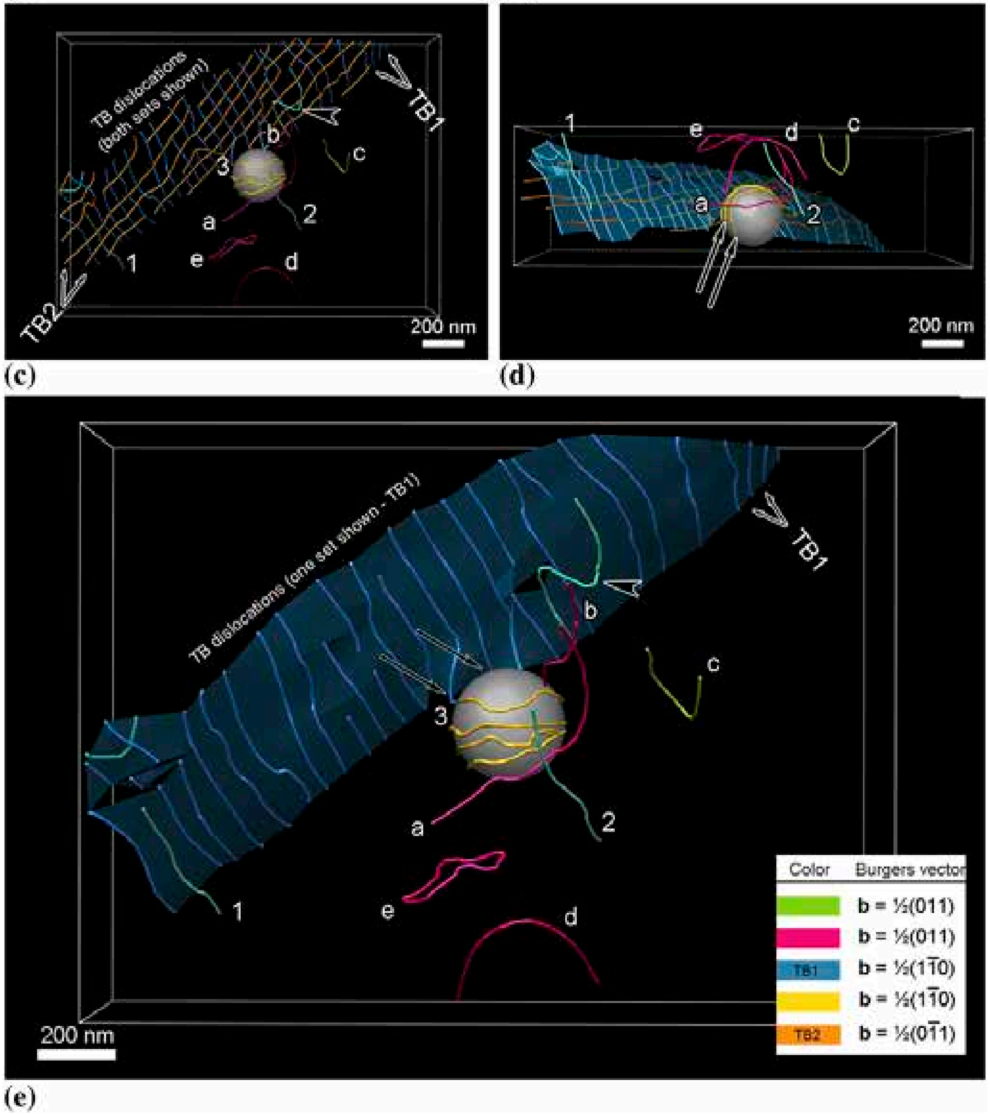

Spatial relationship between the twist boundary, the dislocations, and the particle. (a) and (b) Views from different directions extracted from the tomographic reconstruction. (c)–(e) Views from different directions extracted from the 3D model. In (c), both sets of dislocations in the twist boundary are shown, whereas in (e) one set is removed for clarity and shown with an overlay of the boundary. The “side view” shown in (d) is equivalent to a viewing direction perpendicular to the electron beam, which is normally inaccessible. The arrows indicate dislocations residing in the particle–matrix interface.

[G.S. Liu and I.M. Robertson, J. Mater. Res. **26** (2011)]

Three-dimensional imaging of dislocations in a nanoparticle at atomic resolution

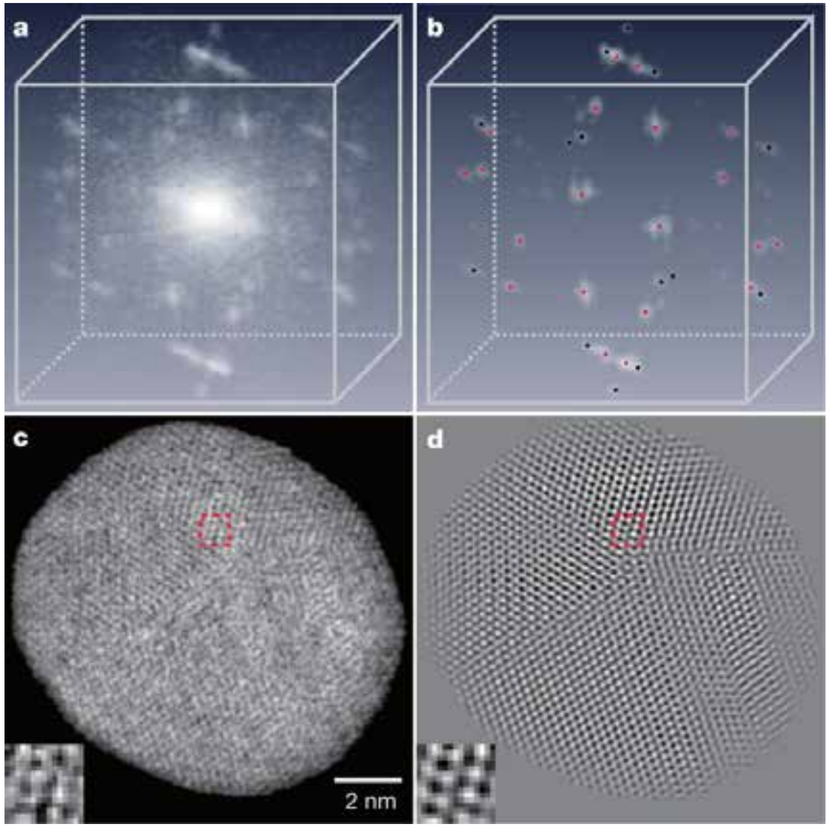

3D reconstruction of a multiply twinned Pt nanoparticle before and after applying a 3D Fourier filter.

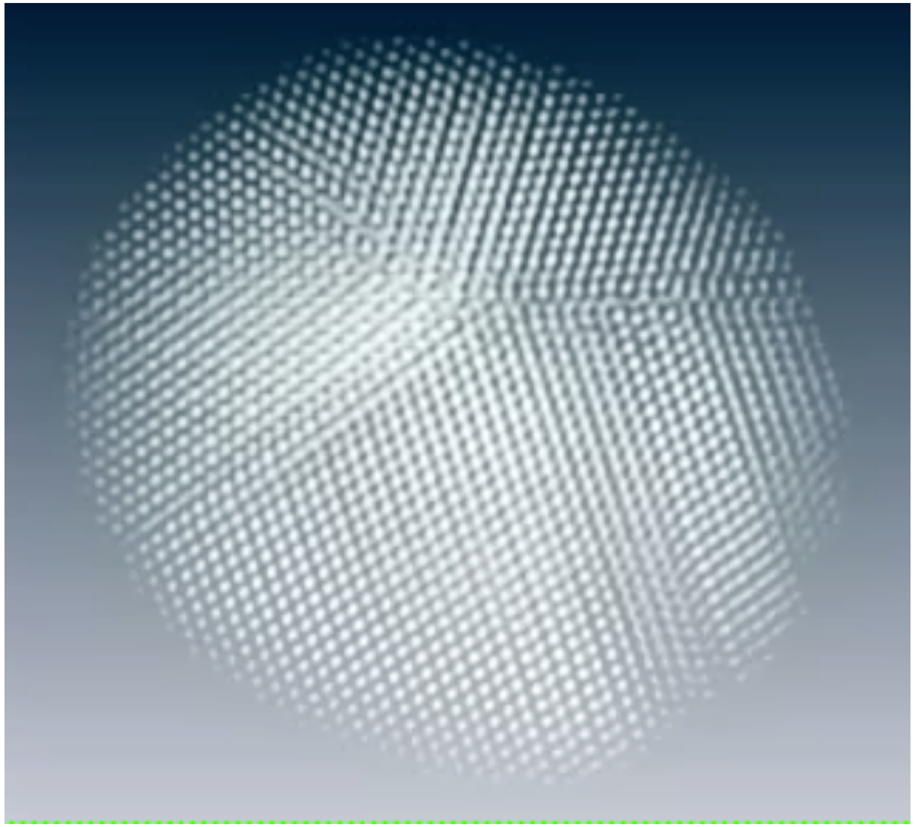

3D volume rendering of the reconstructed Pt nanoparticle after applying a 3D Fourier filter.

C-C Chen *et al.* *Nature* **volume 496**, pages 74–77 (04 April 2013) doi:10.1038/nature12009

Modern Dual-Beam SEM/FIB

Diffraction techniques available in SEM

- Electron backscatter diffraction (EBSD)
  - Conventional orientation microscopy
  - Measurement of micro and macro textures
  - Measurement of elastic stresses
  - 3-dimensional microstructure characterization
- Electron channelling contrast imaging (ECCI)
  - Defect observation (dislocations, stacking faults, strain fields)
- Kossel technique (XRD in the SEM)
  - absolute determination of lattice constants (elastic strains)

Diffraction techniques in SEM

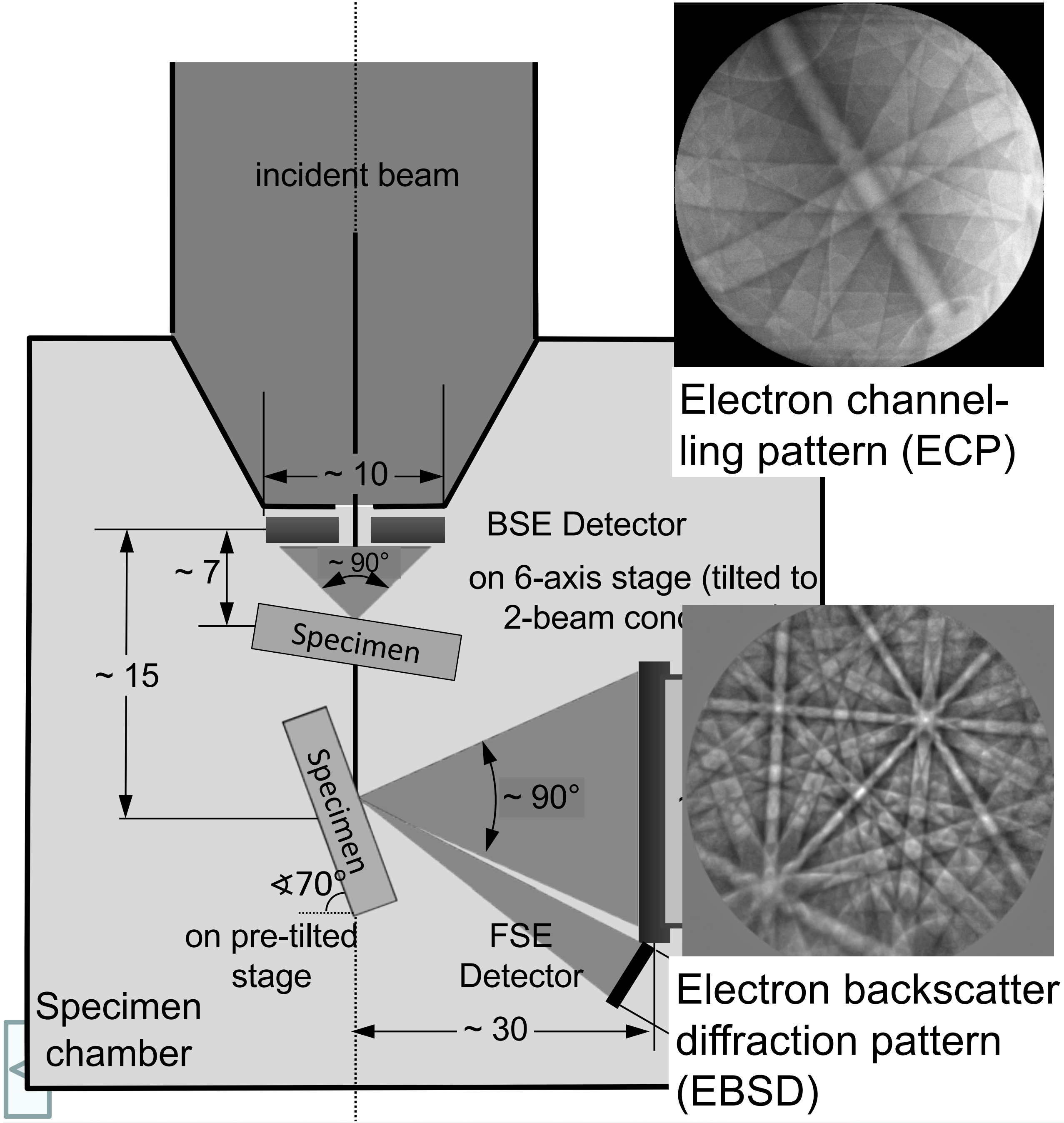

Electron channelling pattern (ECP)

Electron backscatter diffraction pattern (EBSD)

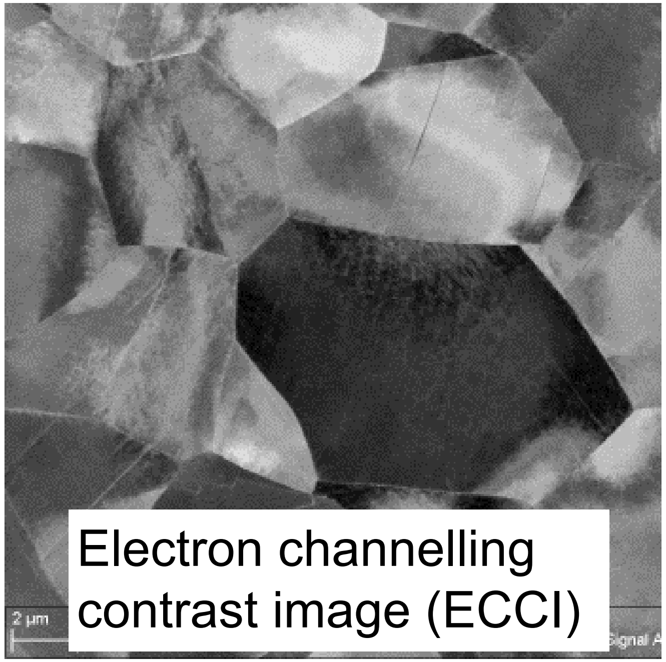

Electron channelling contrast image (ECCI)

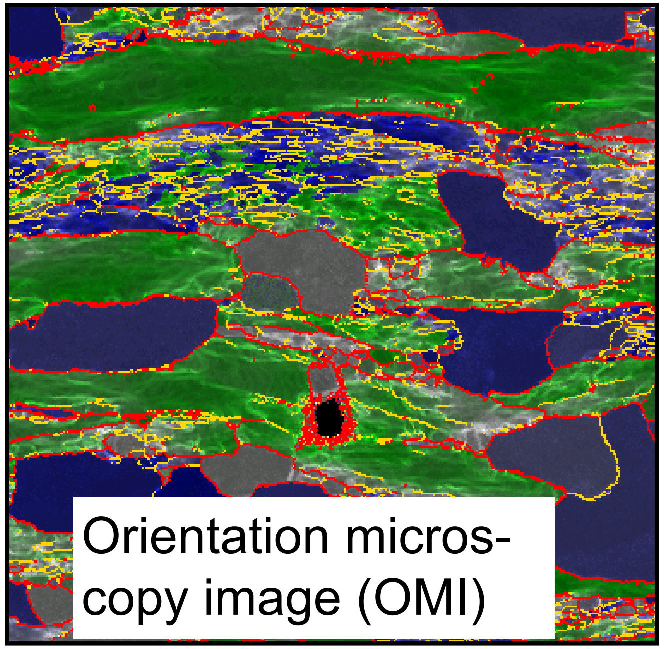

Orientation microscopy image (OMI)

Introduction: Electron backscatter diffraction (EBSD)

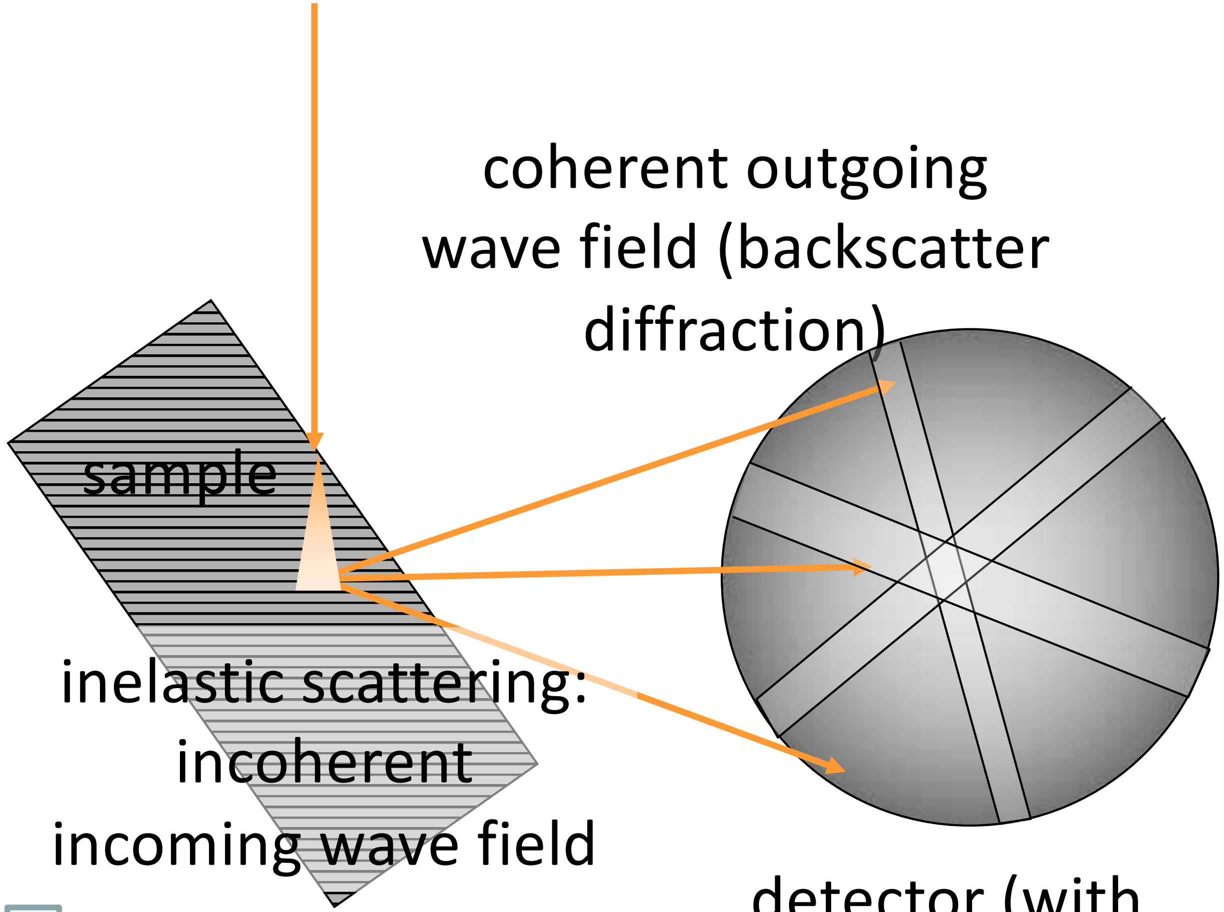

primary
electron beam

coherent outgoing
wave field (backscatter
diffraction)

sample

inelastic scattering:
incoherent
incoming wave field

detector (with
positional sensitivity)

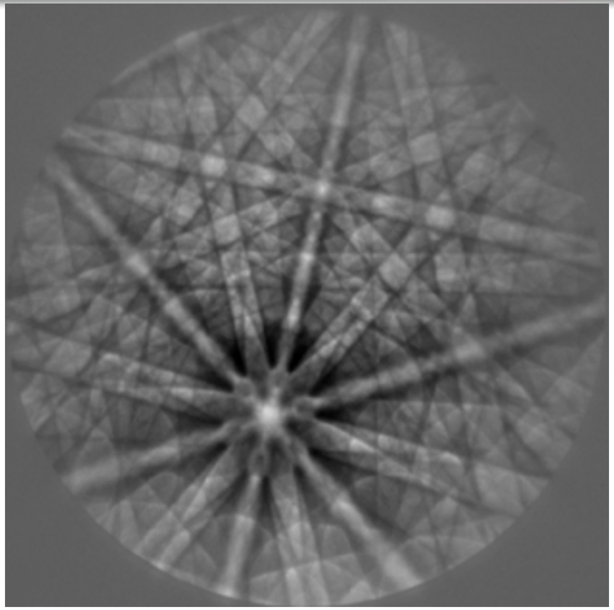

A typical EBSD pattern (Niobium, 15 kV)

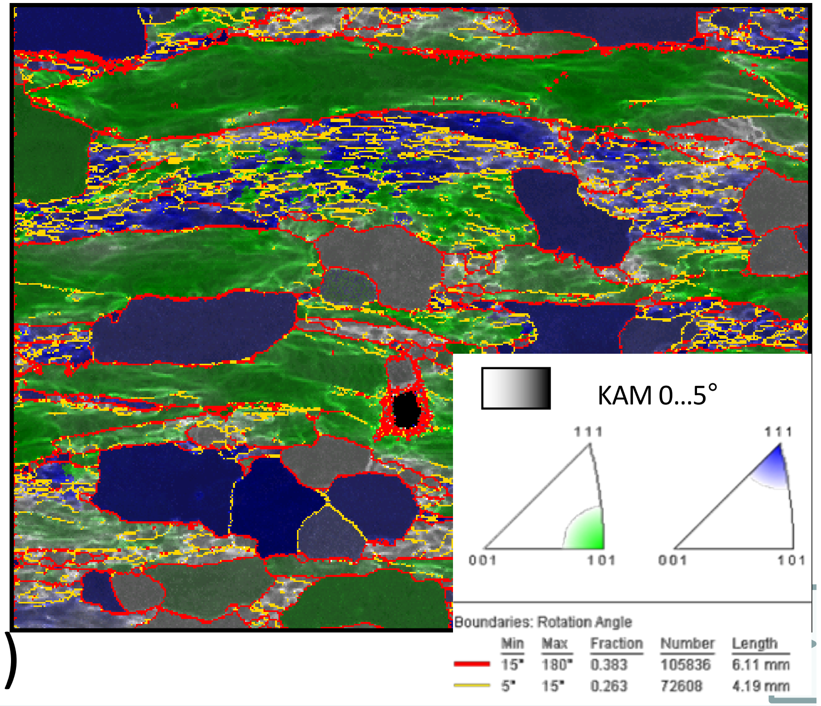

Boundaries: Rotation Angle

	Min	Max	Fraction	Number	Length
🟥	15°	180°	0.383	105836	6.11 mm
🟨	5°	15°	0.263	72608	4.19 mm

Electron channelling contrast imaging (ECCI)

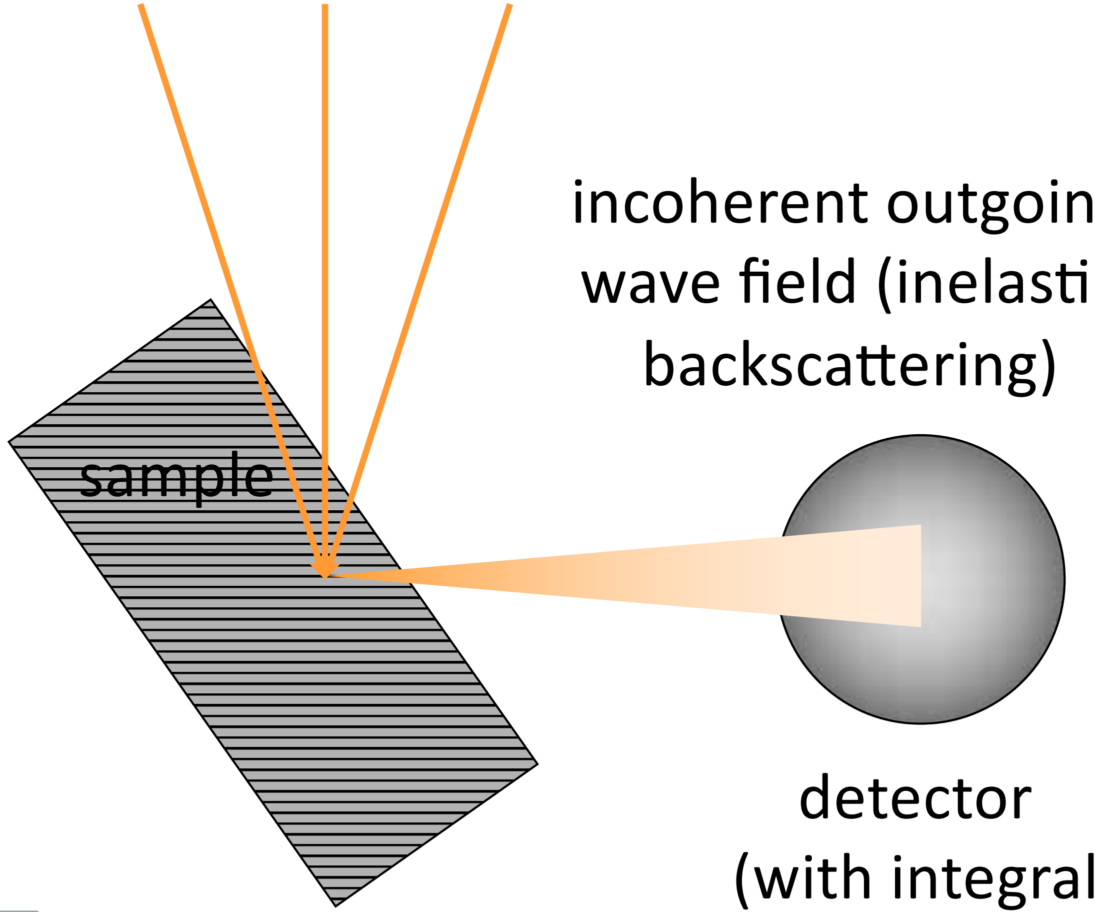

coherent incoming wave field (electron channelling of primary beam electrons)

incoherent outgoing wave field (inelastic backscattering)

detector (with integral sensitivity)

Electron channelling pattern ECP of Cu

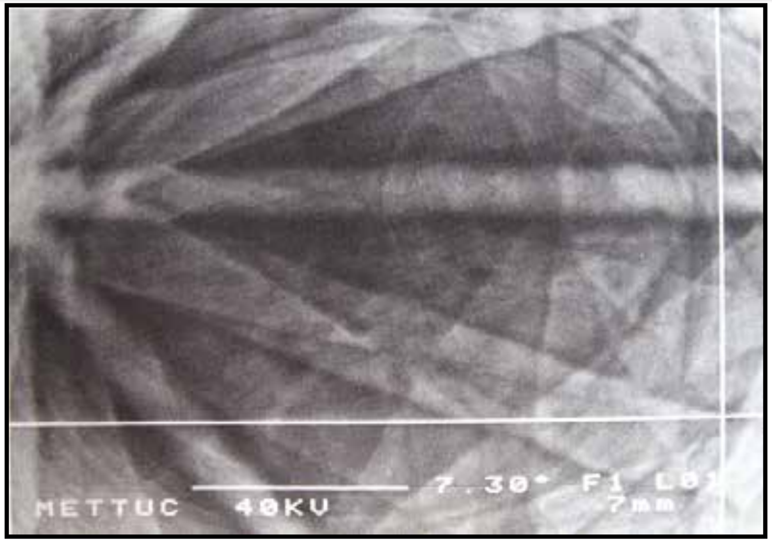

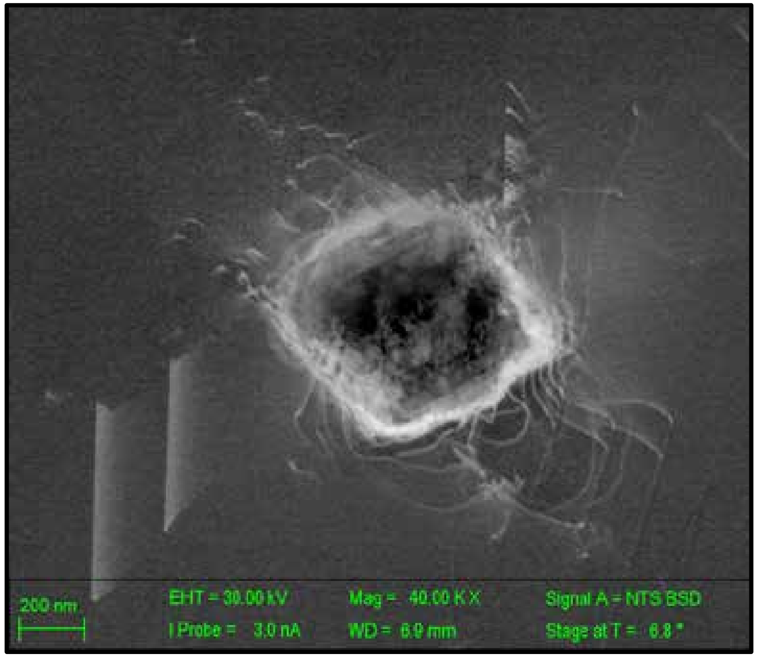

Dislocations and stacking faults in high-Mn austenite

EBSD & EBSD-based orientation microscopy

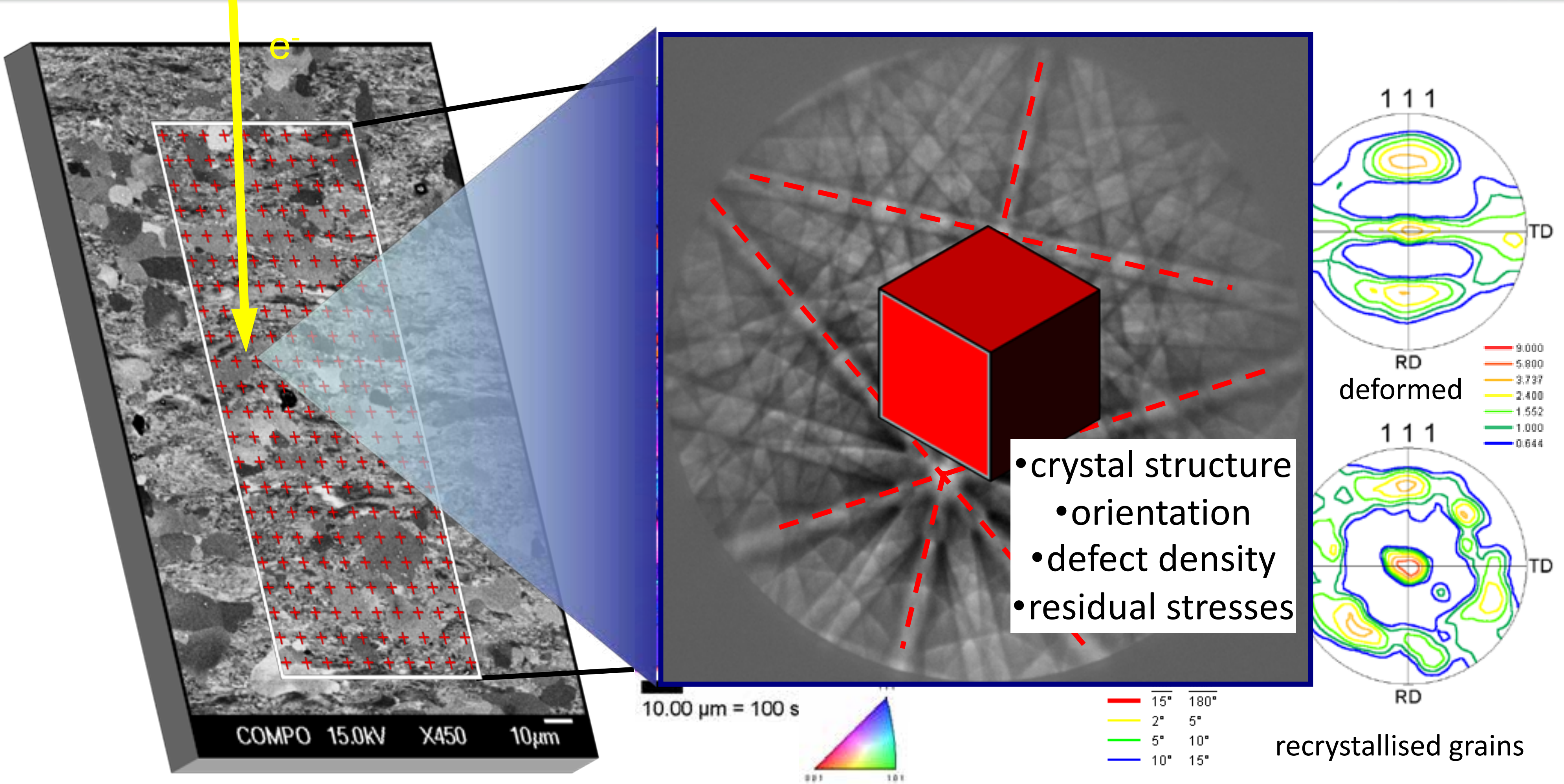

- crystal structure
- orientation
- defect density
- residual stresses

BSEI of a partially recrystallised IF steel

inverse pole figure map

grain boundary character

pole figures

- By nature a “quantitative” technique!
- Spatial resolution: lateral ~ 20 … 300 nm, depth ~ 10 nm
- Angular resolution: conventional 0.5°, special > 0.01°
- Measured area: μm² … cm²

Principle of serial sectioning & orientation microscopy

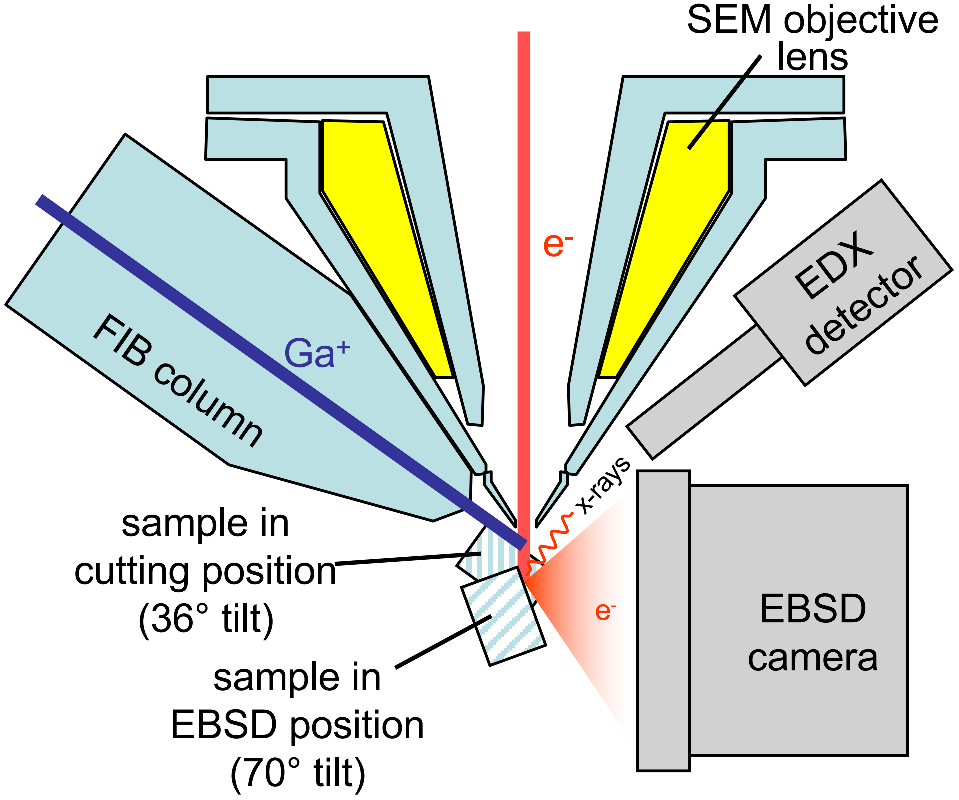

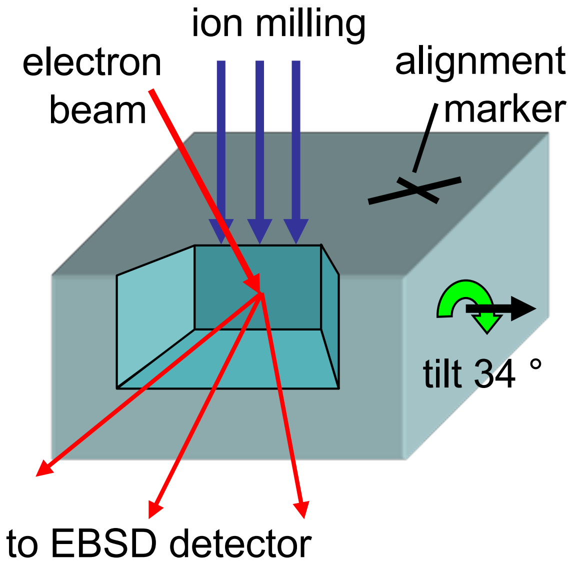

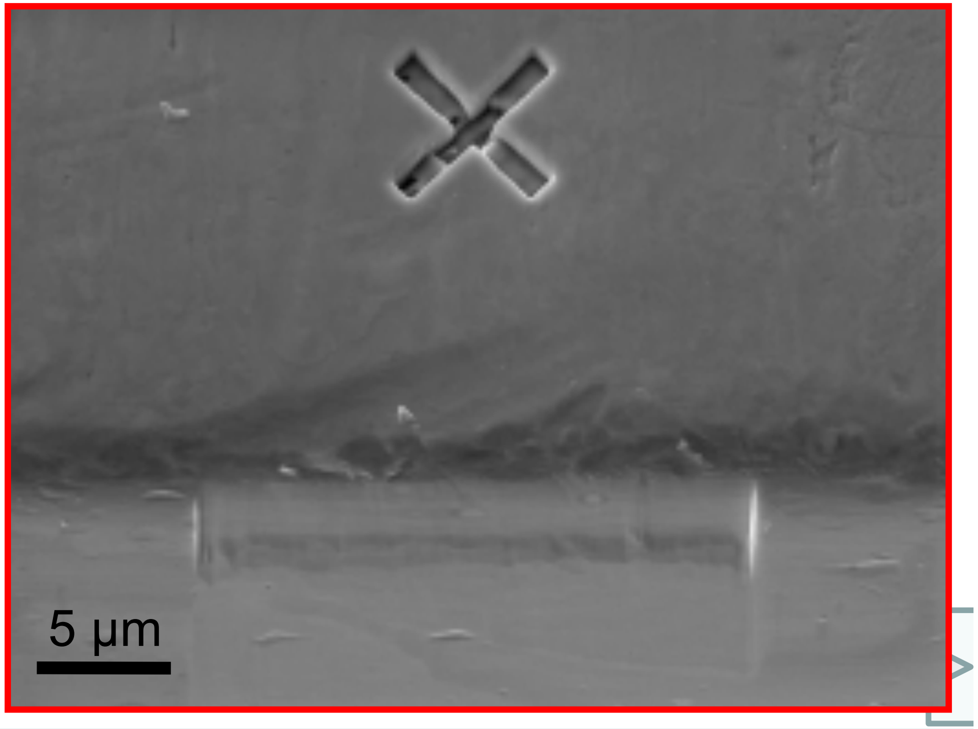

"tilt set-up"
Zaefferer, Wright, Raabe,
Mat. Trans. A (2008)

Comprehensive description of grain boundaries

Khorashadizadeh A, et al. (2011),
Adv. Eng. Mater. 13, 237–244

3D EBSD: serial sectioning & reconstruction with software QUBE (Konijnenberg, Bruker Nano)

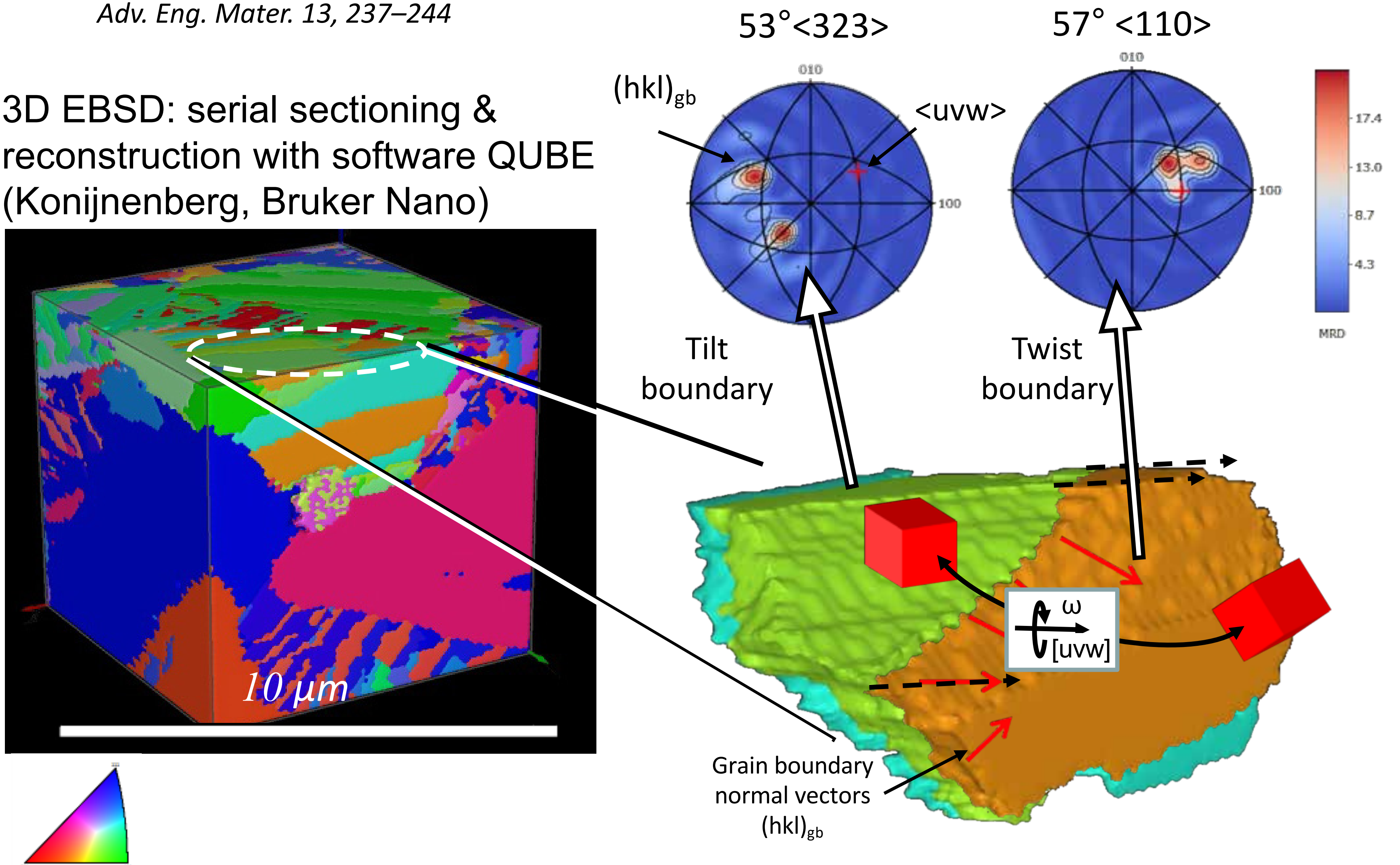

5 rotational parameters: ω (1), <uvw> (2), $(hkl)_{gb}$ (2)

3D reconstruction software QUBE by P. Konijnenberg et al. Mat. Sci. Forum 702-703 (2012) 475-478

Outline

- Introduction:
  - Definition of „microstructures“
  - Electron diffraction techniques in SEM
- Understanding mechanical properties from EBSD observations *(L. Schemmann)*
  - Quantification of dislocation &grain boundary densities
- Individual dislocation observation using ECCI *(D. An, N. Elhami)*
  - Observation and quantification of fatigue structures
- Understanding opto-electronic properties of thin-film solar cell microstructures *(G. Stechmann, P. Konijnenberg)*

Grain boundary network in CdTe solar cell

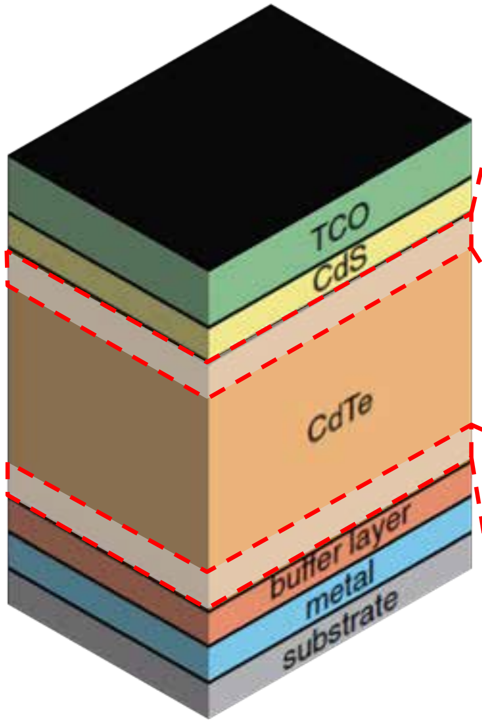

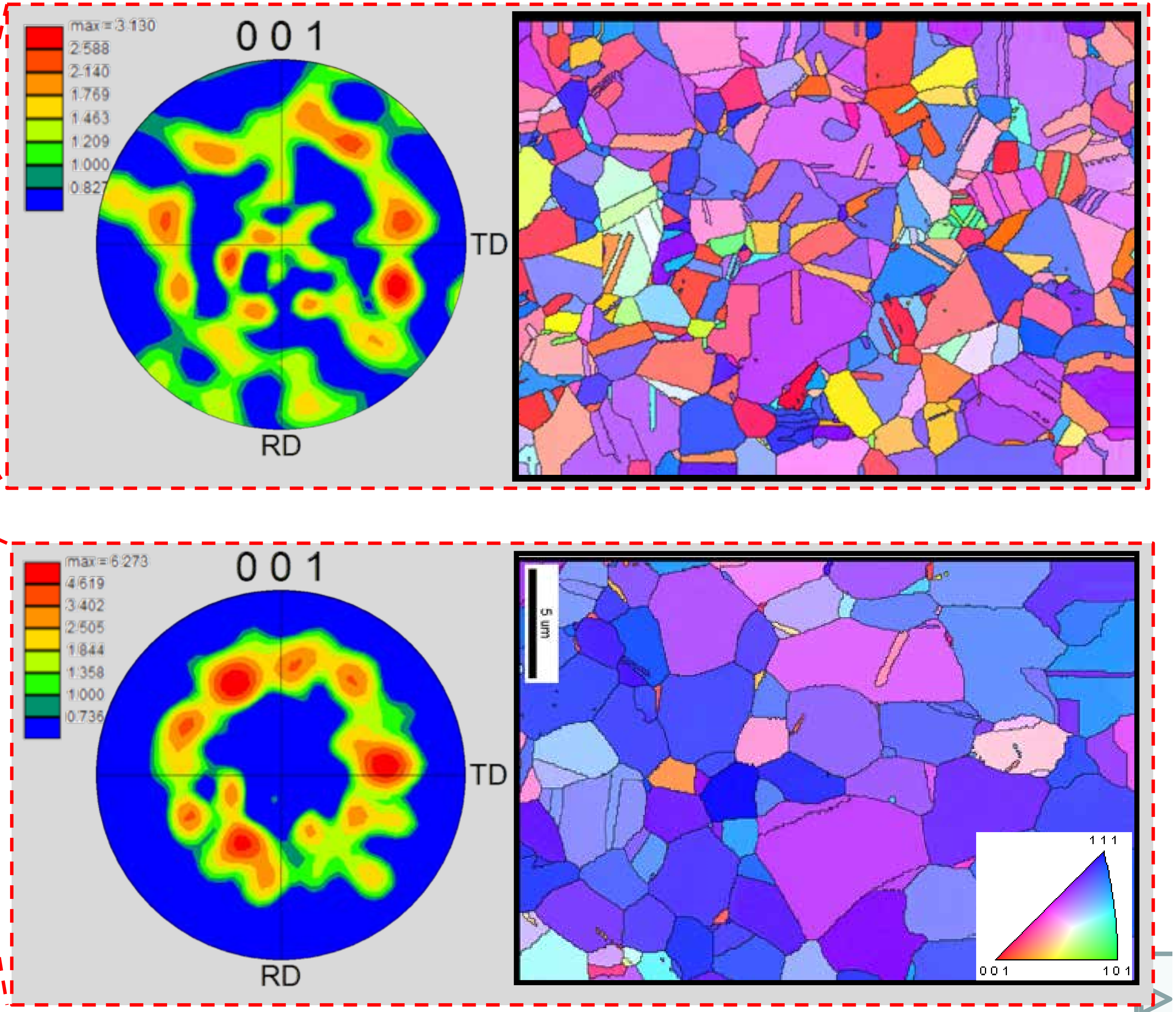

Gretener et al., Prog. Photovolt: Res. Appl., ***2012***

Step size: 70 nm

3D grain boundary structure of CdTe

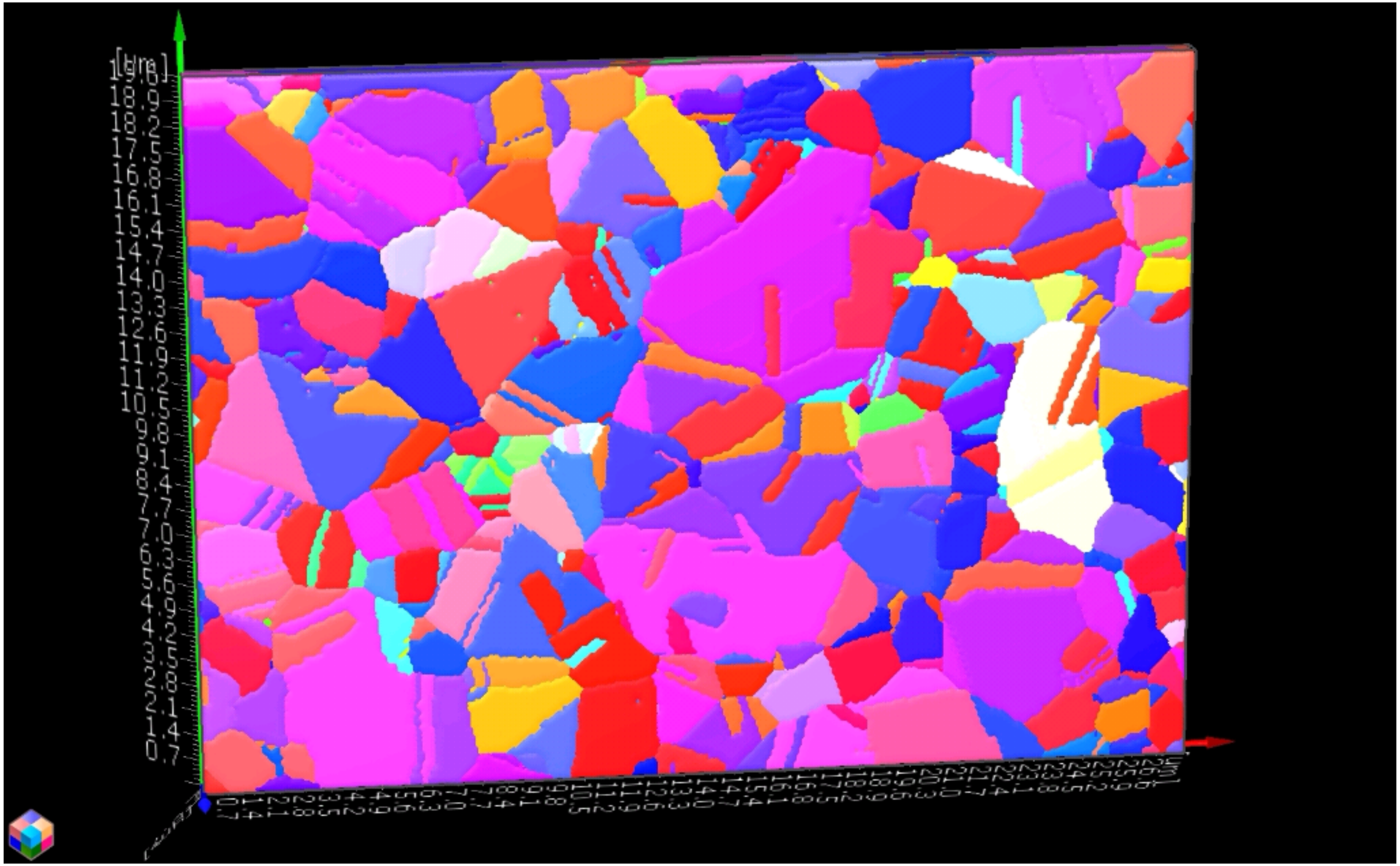

- Now the crystallographic character is fully known – but what are the physical properties of the boundaries?

Chathodoluminescence (CL)

- electron beam creates electron-hole pairs
- electron hole pairs may diffuse in sample
- at non-defected areas: radiative recombination
  - ➢ light emission
- at defects: non-radiative recombination
  - ➢ no light emission

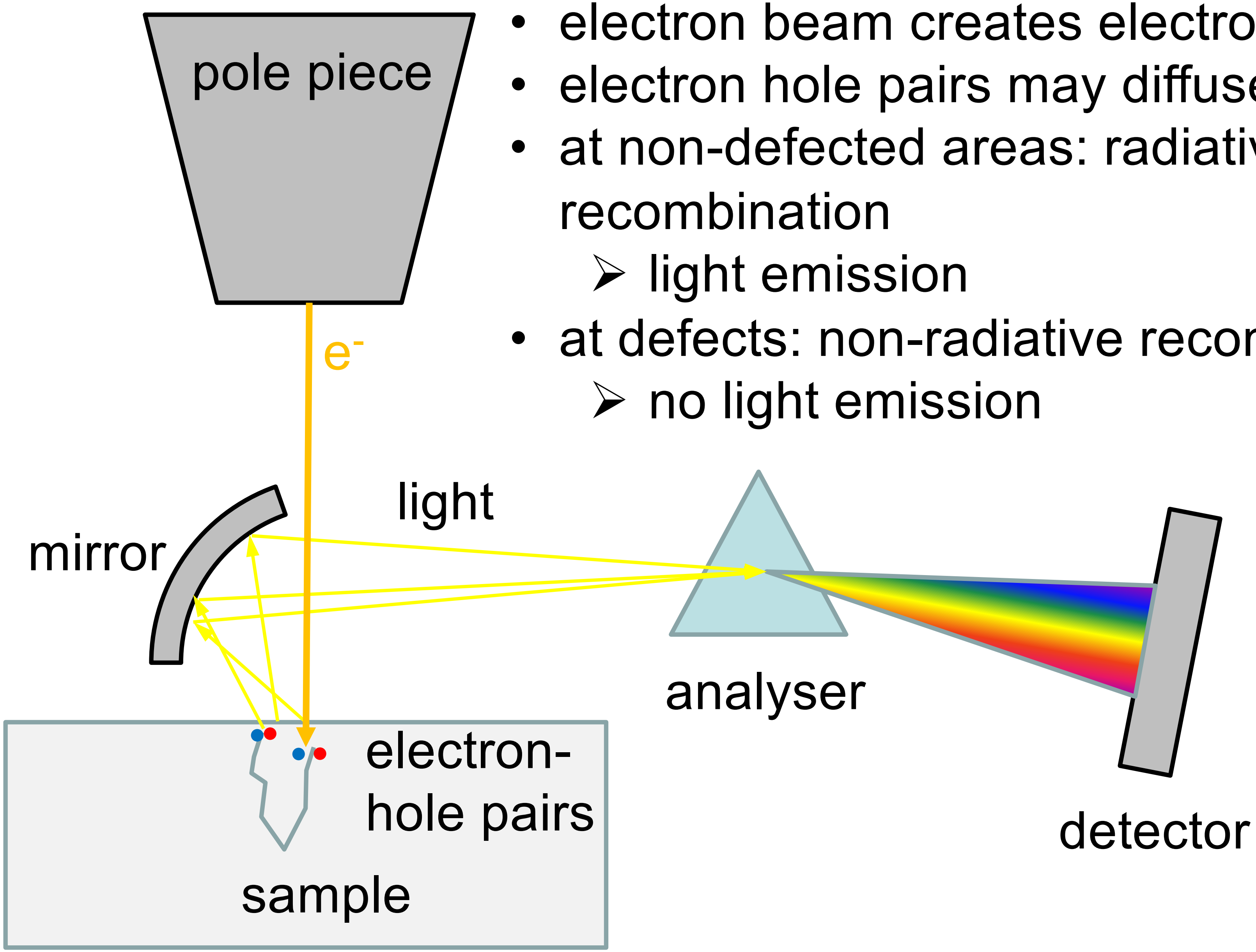

Cathodoluminescence & EBSD

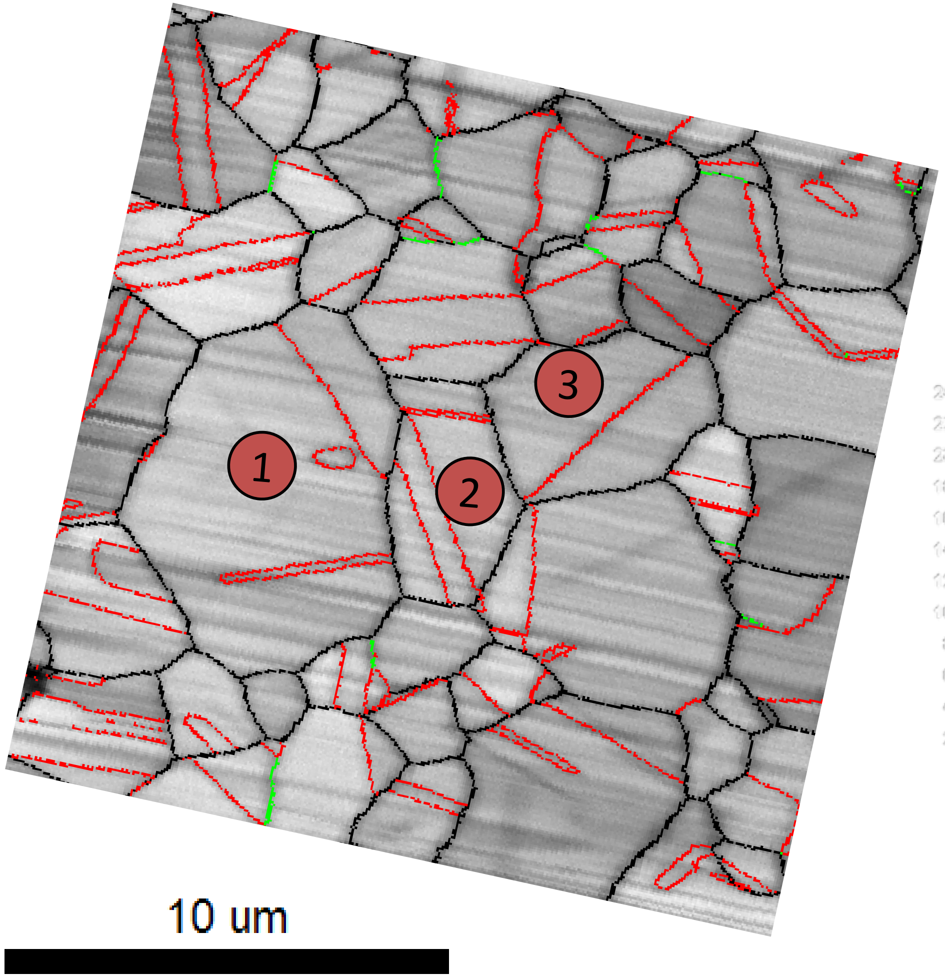

EBSD Image Quality

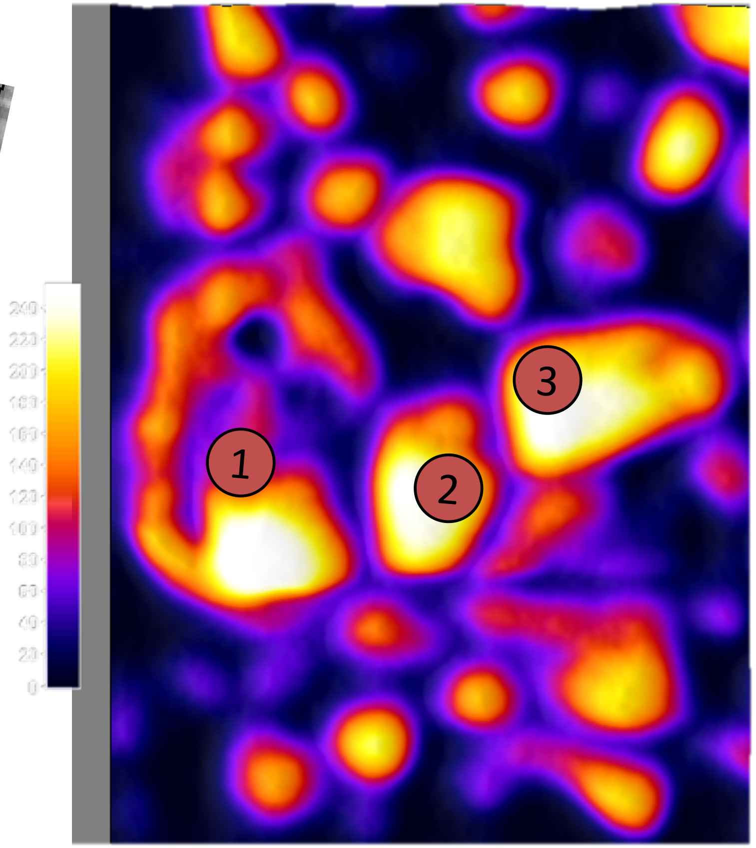

Panchromatic CL

Cathodoluminescence & 3D EBSD

5 Parameters GB characterization combined with CL

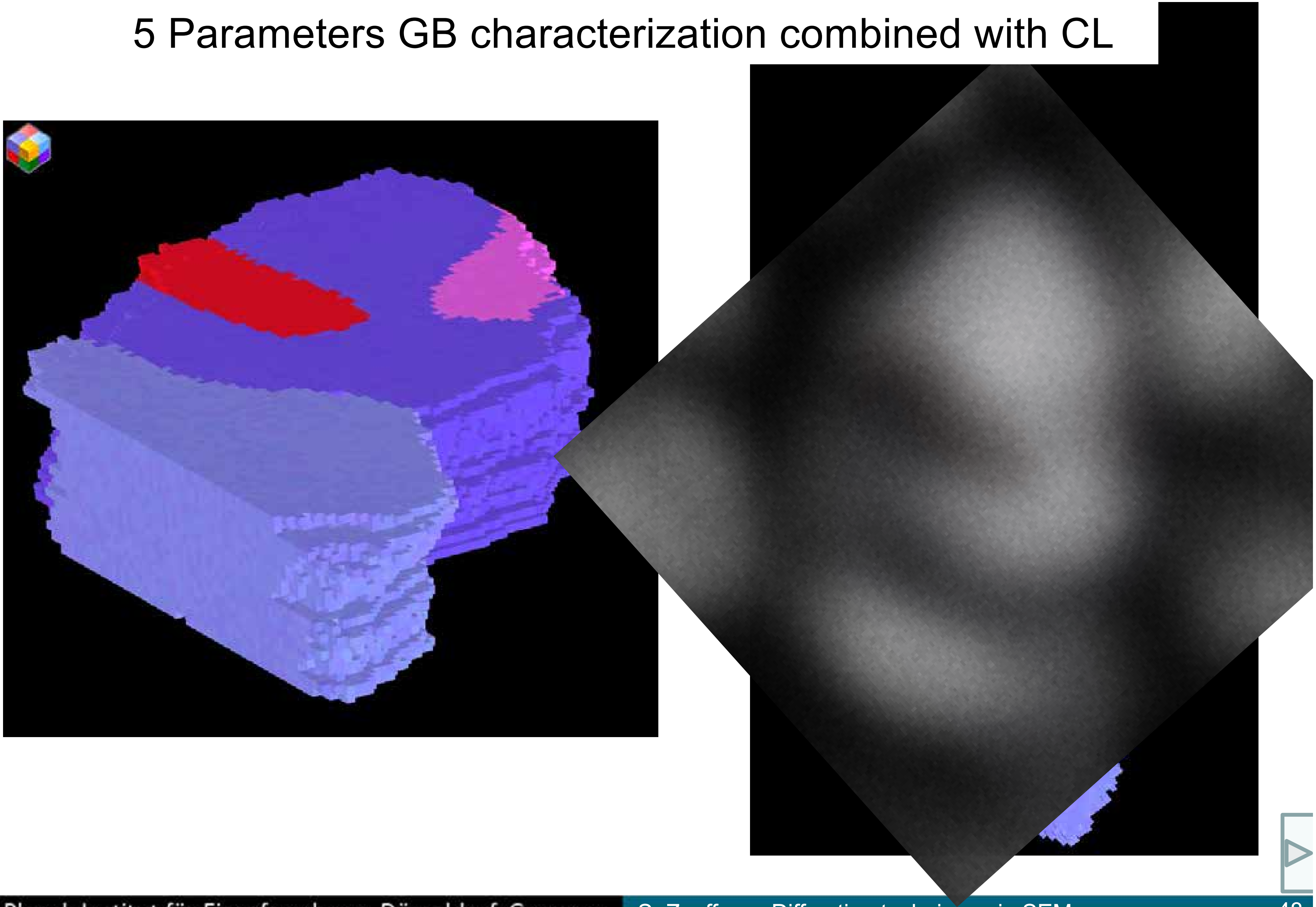

Summary

- The defining difference between various imaging techniques is the source of ‘light’;
- While X-rays and neutrons are convenient for larger volume analysis and *in situ* experiments, Electron Microscopy based techniques are more convenient for high-resolution ***quantitative*** analysis;
    - TEM offers 3D reconstructions from rotation imaging stacks;
    - SEM offers 3D reconstructions from serial sectioning.